

Investigation of a potential therapeutic role for N-oleoylethanolamide and N-linoleoylethanolamide using lymphoblasts deficient in Tafazzin

by

John Zewen Chan

A thesis
presented to the University of Waterloo
in fulfillment of the
requirement for the degree of
Master of Science
in
Kinesiology

Waterloo, Ontario, Canada 2020
©John Zewen Chan 2020

Author's Declaration

This thesis consists of material all of which I authored or co-authored: see Statement of Contributions included in the thesis. This is a true copy of the thesis, including any required final revisions, as accepted by my examiners.

I understand that my thesis may be made electronically available to the public.

Statement of Contributions

JC reviewed the literature, drafted all sections of the manuscript, and created all tables, graphs and figures. RED critically revised all thesis sections and was involved in the conceptualization and organization of the manuscript.

In addition, this work would not have been completed without the help of our collaborators, whom I thank for their contributions:

Gas chromatography experiments:

- Mr. Dan Chalil, MSc, PhD Candidate, University of Waterloo
- Dr. Ken Stark, Professor, University of Waterloo

Transmission electron microscopy experiments:

- Ms. Mishi Groh, MSc, Departmental Technician of Biology, University of Waterloo

Abstract

Barth Syndrome (BTHS) is a rare X-linked genetic disorder caused by mutations in the *TAZ* gene that encodes for the cardiolipin (CL) remodelling enzyme, tafazzin. Patient with BTHS have reduce and altered CL that impacts mitochondrial structure and function leading to numerous disorders, such as cardiomyopathy, skeletal myopathy, and cyclic neutropenia. In prior preliminary work by the Duncan lab, cultured BTHS lymphoblast exhibited major growth deficiencies, and treatment with oleylethanolamine (OEA) partially restored the deficits. OEA is a member of the N-acylethanolamides (NAEs), a group of bioactive signalling molecules produced endogenously when a molecule of phosphatidic acid is hydrolyzed from N-acylphosphatidylethanolamine (NAPE). The aim of this thesis was to investigate the therapeutic potential of OEA and another NAE, linoleoylethanolamine (LEA), in the treatment of BTHS syndrome. Initial experiments examined the effects of OEA and LEA on cell number of BTHS and control lymphoblast cultures. Follow up studies focused on the effects of OEA on BTHS lymphoblasts. This included examining the expression of genes involved in CL using qPCR, the fatty acid composition of CL using gas chromatography and mitochondrial morphology using transmission electron microscopy. In the first study, OEA partially restored the deficits in cell number expansive of five distinct BTHS lymphoblast donors as compared with controls, but LEA, had only minor effects and was not examined further. As for the qPCR analysis, treatment with OEA normalized the increased expressions of the enzyme CDS1 in three BTHS cell lines to a level that was more comparable to healthy controls. OEA did not increase endogenous CL content and failed to normalize the cardiolipin fatty acyl profile of BTHS lymphoblast to match healthy control. Electron microscopy of samples from two distinct BTHS lymphoblast donors had fewer and larger mitochondria as compared with healthy controls. OEA treatment increased

the total mitochondrial number, while decreasing mitochondrial size resulting in mitochondrial network changes. Overall, OEA treatment was only partially successful in restoring BTHS lymphoblast growth while LEA was not. The effect of OEA on BTHS lymphoblast growth appears to be mediated by the direct modulation of the mitochondria. Future studies should examine pathways involving mitochondrial biogenesis and fission, specifically the expression of PGC-1 α and DRP1 which may be new targets for BTHS treatment.

Acknowledgements

First, I would like to thank my supervisor, Dr. Robin Duncan for your undying support and positivity. Your guidance has helped me tremendously over the past two years and has really given me the confidence and belief to succeed in academia. Thank for very much for putting up with all of the short to long talks we have in your office whether it be about research, life-advice or personal issues. They really mean a lot to me and has kept me looking forward to working with you for years to come.

Thank you to our collaborator Mishi Groh for your hard work and dedication. Despite your busy schedule, the countless hours you have put into sectioning and imaging our Barth and healthy lymphoblast lines provides a very important piece to answering our research question.

Thank you to the many lab mates and researchers within the physiology departments. You have all made me feel very welcomed and blessed to be working in such a caring environment and I am pleased to be able to call many of you my friends. Thank you to Joey Hung who is always looking out for me and our many talks after failed experiments; to Ashkan Hashemi, who is like a mentor figure to me and mentored me to become a more independent researcher; to Kalsha Da Silva for your kind nature and being the sibling that I never had; and Fernanda for your troubleshooting skills.

Thank you to Leung Choy Education Trust, for your continuous support over my undergraduate education period. Your faith in me has allowed me to carry on my dreams in pursuing research.

Finally, and most importantly, I would like to thank my mom and dad who are the most important people in my life. Dad, the countless hours that you have put into training me to become a tennis athlete has taught me the values of hard work and patience and I am forever grateful. Mom, thank you for supporting me all these years, whether it be financially or emotionally, you have always been there for me and I will give all my efforts to pursue my goals to make you proud.

Dedication

This thesis is dedicated to my parents Eric Chan and Sun Ying.

Table of Contents

<i>Author's Declaration</i>	<i>ii</i>
<i>Statement of Contributions</i>	<i>iii</i>
<i>Abstract</i>	<i>iv</i>
<i>Acknowledgements</i>	<i>vi</i>
<i>Dedication</i>	<i>vii</i>
<i>List of Figures</i>	<i>x</i>
<i>List of Tables</i>	<i>xii</i>
<i>List of Abbreviations</i>	<i>xiii</i>
Chapter One: Introduction	1
Barth Syndrome (BTBS).....	1
Neutropenia and lymphopenia	2
Chapter Two: Background	4
General background	4
Function of CL in the mitochondria	5
Cardiolipin Biosynthesis/remodeling	7
Characterisation of BTBS and healthy cell fatty acyl composition	9
Differences between BTBS and healthy lymphoblast in mitochondrial function and ultrastructure	12
Therapeutic strategies using N-acylethanolamines (NAEs).....	14
Chapter Three: Thesis Study I – Effects of OEA and LEA on BTBS and control lymphoblast cell number	17
Introduction and Study Rationale.....	17
Objectives and Hypothesis	20
Method:	21
Statistical Analysis:	22
Results	23
Discussion	28
Chapter Four: Thesis Study II – Effects of OEA on CL metabolism and composition	31
Study Rationale	31
Objectives and Hypothesis:	33
Methods:	34
Statistical Analysis:	38
Results:	39

Discussion:	45
<i>Chapter Five: Thesis Study III – Effect of OEA on BTHS Lymphoblast Mitochondrial Number, Size, and Morphology</i>	48
Study Rationale	48
Objectives and Hypothesis	50
Methods:	51
Results:	53
Discussion:	57
<i>Chapter Six: Thesis Summary, Integration, and Conclusion</i>	62
<i>References</i>	72
<i>Appendices</i>	83

List of Figures

Figure 1:	Cardiolipin Structure	4
Figure 2:	Cross-sectional view of a lymphoblast mitochondria derived from a 10-year old male Barth patient	13
Figure 3:	Effect of OEA and LEA on lymphoblast cell number over 4 days of growth	25
Figure 4:	Individual donor responses to the effect of OEA treatment for 4 days on cell number	26
Figure 5:	Individual donor responses to the effect of LEA treatment for 4 days on cell number	27
Figure 6:	Expression of related cardiolipin biosynthetic/remodelling genes in vehicle and OEA treated healthy and BTHS lymphoblasts	42
Figure 7:	Preliminary cardiolipin analysis of a single set of BTHS and healthy lymphoblasts (GM22163 & AG14750), treated with OEA or vehicle	43
Figure 8:	Fatty acyl profile of CL isolated from a single set of BTHS and healthy lymphoblasts (GM22163 & AG14750) treated with or without OEA	44
Figure 9:	Transmission electron microscopy images of lymphoblasts derived from BTHS (GM22192 & GM22163) and healthy (AG15022 &AG14750) donors	55
Figure 10:	Additional analysis of the transmission electron microscopy images of lymphoblasts derived from two sets of BTHS (GM22192 & GM22163) and healthy (AG15022 &AG14750) donors, treated with vehicle or OEA	56

Figure 11:	Proposed mechanisms for the effects of OEA to increase BTHS lymphoblast cell number	61
App. Fig. 1:	Technical replicates of the growth data of each individual BTHS and healthy lymphoblast donors, treated with OEA or vehicle	83
App. Fig. 2:	Technical replicates of the growth data of each individual BTHS and healthy lymphoblast donors, treated with LEA or vehicle	84
App. Fig. 3:	Preliminary cardiolipin analysis of a single BTHS lymphoblasts cell line (GM22192), treated with OEA or vehicle.	86
App. Fig. 4:	Fatty acyl profile of CL isolated from a single BTHS lymphoblast line (GM22192) treated with or without OEA	87
App. Fig. 5:	Relatively lower protein levels of cleaved caspase 7 and cleaved PARP in BTHS lymphoblasts compared to healthy controls	88

List of Tables

Table 1:	Relative fatty acyl composition of lymphoblast cardiolipin	12
Table 2:	Individual Barth and healthy donor characteristics from Coriell Biorepository	22
Table 3:	List of human primer sequences used in qPCR experiments	36
Table 4:	Summary of key findings	71
App. Table 1:	Absolute mass of individual fatty acyl species within the CL of GM22163 (BTHS) and AG14750 (healthy) in micrograms per 10 million cells ($\mu/10^7$ cells)	85

List of Abbreviations

(q)PCR – quantitative polymerase chain reaction
ADP – adenosine diphosphate
AGPAT – acylglycerolphosphate acyltransferase
ALCAT1 - acyl-CoA:lysocardiolipin acyltransferase
ANT – adenine nucleotide translocator
ATP – adenosine triphosphate
BID – BH3 interacting domain death agonist
BSA – bovine serum albumin
BTHS – Barth Syndrome
Caspase - cysteine-dependent aspartate-directed proteases
CB1 – cannabinoid receptor type 1
CB2 – cannabinoid receptor type 2
CCCP – carbonyl cyanide *m*-chlorophenyl hydrazine
cDNA – complementary DNA
CDP-DAG – cytidine diphosphate diacylglycerol
CDS - phosphatidate cytidyltransferase
CL – cardiolipin
Complex I – NADH: ubiquinone oxidoreductase
Complex II – succinate dehydrogenase (SDH)
Complex III – coenzyme Q – cytochrome c reductase
Complex IV – cytochrome c oxidase
CTP – cytidine triphosphate
DCM – dilated cardiomyopathy
DRP1 – dynamin-1-like protein
DDH₂O – double distilled water
DLCL – dilysocardiolipin
E/A – Epon-Araldite
ETC – electron transport chain
ETOH – ethanol
FBS – fetal bovine serum
G3P – glycerol-3-phosphate
GAPDH - glyceraldehyde 3-phosphate dehydrogenase
GC – gas chromatography
GPAT – glycerolphosphate acyltransferase
GPR119 - G protein-coupled receptor 119
GPR55 - G protein-coupled receptor 55
IBM – inner boundary membrane
IMM – inner mitochondrial membrane
LA – linoleic acid
LEA - linoleoylethanolamide
LEA – linoleoylethanolamide
lysoPA - lysophosphatidic acid
MGA – methylglutaconic aciduria
MLCL – monolysocardiolipin

MLCL AT-1 - monolysocardiolipin acyltransferase 1
MOMP – mitochondria; outer membrane permeabilization
mRNA – messenger ribonucleic acid
mRNA – messenger RNA
NAEs - N-acylethanolamines
NAPE – N-acylphosphatidylethanolamine
NAPE-PLD – N-acylphosphatidylethanolamine phospholipase D
NAT - N-acyltransferase
OEA – oleoylethanolamide
OEA – oleoylethanolamide
OMM – outer mitochondrial membrane
OPA1 – optic atrophy protein
OsO₄ – osmium tetroxide
PA – phosphatidic acid
PARP – poly (ADP-ribose) polymerase
PC – phosphatidylcholine
PE – phosphatidylethanolamine
PEA – palmitoylethanolamide
PG – phosphatidylglycerol
PGP - phosphatidylglycerol phosphate
PGPS - phosphatidylglycerol phosphate synthase
PIC – protease inhibitor cocktail
PLA1s – phospholipase A1s
PLA2s – phospholipase A2s
PPAR α - peroxisomal proliferator-activated receptor-alpha
PTPMT1 - protein tyrosine phosphatase, mitochondrial 1
RNA – ribonucleic acid
ROX – residual oxygen consumption
RPMI – Roswell Park Memorial Institute
SDS – sodium dodecyl sulfate
SDS-PAGE - sodium dodecyl sulfate-polyacrylamide gel electrophoresis
SEA – stearoylethanolamide
t-BID truncated BH3 interacting domain death agonist
TEM – transmission electron microscopy
TLC – thin layer chromatography
TMPD – tetramethylphenylenediamine
TRPV1 - transient receptor potential cation channel subfamily V member 1

Chapter One: Introduction

Barth Syndrome (BTHS)

Barth syndrome (BTHS) is a very rare X-linked recessive disorder with an incident rate of approximately one in every 300 000 to 400 000 births, and only ~300 identified cases worldwide [1]. After the first reported case by Dr. Peter Barth in 1983, studies examining patients with BTHS have identified more than 200 unique mutations in the *TAZ* gene located on the distal portion of chromosome Xq28 [2, 3]. A majority of these mutations are small insertions, deletions and missense mutations, but entire exon/gene deletions have also been evident as well [3]. *TAZ* gene mutations encode for a less-functional Tafazzin enzyme, which decreases its ability to remodel monolysocardiolipin into linoleoyl-enriched CL [4].

The functional implications of *TAZ* deficiency vary depending on tissue, with the most severe mitochondrial disturbances occurring in organs with a high content of linoleate-enriched CL, such as heart and skeletal muscle, which contains ~70-80% tetra-linoleoyl CL [4]. However, impairments are also observed in other tissues as well, since 18:2 n-6 is proportionately significant in kidney (~61%), some immune cell types (~49%), and other organs [45, 46]. Therefore, patients with BTHS have a decrease in endogenous CL levels in many tissues, with a concomitant accumulation of monolysocardiolipin that is coupled to their significant reduction in CL remodeling capacity [4, 5].

As a result of *TAZ* deficiency, most patients manifest symptoms of dilated cardiomyopathy within one year of birth, leading to progressive heart failure [6]. BTHS is also characterised by neutropenia, skeletal myopathy, prepubertal shortness in stature with delayed puberty that results in an often excessive and rapid growth spurt, 3-methylglutaconic aciduria,

and some varying degree of cognitive impairment, although many individuals with BTHS complete advanced study [1, 7].

Neutropenia and lymphopenia

One of the major symptoms of BTHS is neutropenia, caused by the sporadic declines in neutrophil concentration, often reaching levels below 1.5 ± 10^9 cells per liter of peripheral blood [8]. This reduction in neutrophil number affects up to 90% of BTHS patients and can lead to deadly systemic infections by bacteria or yeast that are normally harmlessly resident in the gastrointestinal tract and on the skin [7]. While the pathology of BTHS-related neutropenia is not fully understood, there are several proposed mechanisms that may explain this detriment. First, it was suggested by Van & Kuijpers (2009) that the decrease in neutrophil concentration was due to the externalization of phosphatidylserine (PS), which lead to an increased clearance of neutrophils by tissue macrophages [9]. However, this theory was disproven as the co-incubation of BTHS neutrophils with macrophages did not decrease the total neutrophil count despite increased Annexin V binding [10]. Instead, recent studies suggest that BTHS neutropenia is unlikely to be directly caused by a deficit in neutrophils, *per se*, since BTHS neutrophil function was shown to match that of healthy controls, but rather due to a deficiency in precursor cells [8, 11]. Individuals with BTHS neutropenia have accelerated myeloid progenitor cell apoptosis and a decrease in myeloid maturation [8, 11]. Given this information, many BTHS patients take the drug NEUPOGEN® to stimulate neutrophil progenitor cell proliferation and maturation, which has proven successful in increasing circulating neutrophil levels.

Until recently, most of the clinical studies on BTHS-related immune function focused specifically on neutrophils and neutropenia [7, 9-12]. However, results communicated during a

recent BSF Scientific and Medical Symposium suggested that the immune deficiencies in BTHS are not limited to neutropenia [13, 14]. Unpublished data on Tafazzin knockout mice showed evidence of a reduction in the numbers of lymphocytes of both T and B lineage, which was indicative of lymphopenia in this model [13]. This suggests that BTHS patients may also have difficulty initiating an immune response through adaptive immunity to fight off bacterial or viral infections. Since research on BTHS-related lymphopenia is still very limited, this thesis aims to examine cultures of BTHS patient-derived lymphoblasts, and a potential new therapeutic treatment for BTHS lymphopenia, in the hopes that it could help reverse immunological deficits. To help answer this question, a BTHS lymphoblast cell line was chosen as the study model, since it is an precursor cell that can give rise to lymphocytes of both the T and B lineage. Due to the rare occurrence of BTHS, sample collections from patients have been highly limited over the years. As a result, BTHS lymphoblast were also chosen on the bases that it was one of the few cell lines that were readily available [15].

The primary focus of this thesis was to access the capacity of oleylethanolamine (OEA) or linoleoylethanolamine (LEA) as potential therapeutic agents in the treatment of the immunological deficits presented in BTHS. To elucidate this, three objectives were investigated, which examined the effects of treatment on BTHS lymphoblast cell growth, CL content and composition, and mitochondrial morphology. OEA and LEA, are part of a group of bioactive lipids known as NAEs, which will be further discussed in greater detail in chapter two.

Chapter Two: Background

General background

Cardiolipin (CL), first isolated from a sample of bovine heart in 1942, is a type of glycerophospholipid found predominately in the inner membranes of mitochondria [16, 17]. Despite “cardio” in its nomenclature, this lipid is synthesized ubiquitously across all mitochondrial mammalian tissues, where it is essential for the proper functioning and structure of the mitochondria [18]. This includes performance of oxidative phosphorylation, formation of mitochondrial ultrastructure, and participation in mitochondria-related apoptosis [19, 20]. In terms of general structure, CL is unique compared to other glycerophospholipids such as phosphatidylethanolamine [PE] and phosphatidylcholine [PC], since it contains four, rather than two, fatty acyl side chains, with two glycerophospholipids linked by a glycerol molecule (**Fig. 1**) [19]. Given the importance of CL to mitochondrial function, deficiency in, or changes to CL composition are associated with a variety of chronic diseases ranging from Parkinson’s disease, to cardiovascular diseases, to hyperthyroidism, and some cancers, and also play a role in reduced energy production in normal aging [21-27]. Moreover, at least one disease, Barth Syndrome, is known to result from genetic defects in CL synthesis and remodeling. Understanding the cellular regulation of CL is therefore of importance in health and disease.

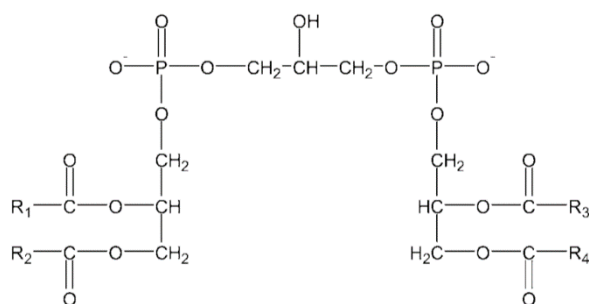


Figure 1: Cardiolipin Structure

Figure adapted from Vaz et al. (2003). Cardiolipin contains a single glycerol head group esterified onto two phosphatidyl moieties.

Function of CL in the mitochondria

A major role of CL within the mitochondria involves the organization of mitochondrial cristae [28]. Cristae are the inward foldings of the inner mitochondrial membrane (IMM), which allow for more surface area to provide greater space for the generation of ATP [28]. A typical crista structure contains three distinct features: a crista junction, stalk, and tip [28]. The junction is a region where the crista extends inwards from the inner boundary membrane (IBM) perpendicular to the outer mitochondrial membrane (OMM) [28]. The stalk is the longest portion of the crista, which spans from the junction to the tip [28]. Finally, the tip is a segment that serves as a “dome-shaped” cap and is the curved region of the crista [28]. Since CL possesses two phosphatidyl moieties that share a common glycerol head group, it is innately a “cone-shaped” molecule [29]. Due to this, CL is enriched in the negative curved regions of the inner mitochondrial membrane (IMM) lipid bilayer, facing the mitochondrial matrix side [28]. This helps relieve the stress/tension associated with high membrane curvature, such as occurs at the cristae tip [28]. In addition, the cristae tip contains a dense network of dimerized/oligomerized ATP synthase molecules, which form “ribbon-like” rows to further promote membrane curvature [30, 31]. CL is essential in the oligomerization and dimerization of ATP synthase, thus playing an additional role in the organization of cristae [31].

As the site of ATP synthase complex assembly, CL also plays a critical role in cellular respiration [19]. CL is tightly bound to all electron transport chain complexes (Complex I, II, III, IV), and is critical to their activity, function, and stability [32-35]. For example, the complete removal of CL from cytochrome C oxidase in Complex IV decreased electron transport capacity by nearly 50%, and also caused specific subunits within its quaternary structure to dissociate [34]. Imaging studies using a single particle cryoelectronic microscopy have also revealed an

abundance of CL between individual complexes of the electron transport chain, which suggests that it is involved in the assembly of respiratory proteins into super-complexes [36]. The presence of CL is also vital to the proper functioning of mitochondrial substrate carriers, including the ADP/ATP translocase, also called the adenine nucleotide translocase (ANT), and the mitochondrial phosphate carrier SLC25A3 [37, 38].

In addition to the many roles of CL in cristae morphology and energy production, CL is also directly involved with mitochondrial dynamics. It plays a part in both fusion and fission processes [39], such that, the direct interaction between Dynamin-related protein 1 (DRP1) and CL has been noted to enhance the GTPase activity of DRP1 and causes it to assemble into higher order oligomer structures [40, 41]. This allows for the facilitation of inner and outer membrane constriction and division, which are two important events during mitochondrial fission [40]. As for mitochondrial fusion, CL was shown to interact with the optic atrophy 1 (OPA1) protein, in a mechanism that involves the direct heterotypic binding of L-OPA1 from one side of the IMM to the opposing side of the IMM with CL [42, 43]. Fusion of the OMM is mediated by the mitofusins (MFN1 and MFN2) [44]. Since no studies have found a direct effect between CL and MFN1 and MFN2 function, this suggests that CL is unlikely to be involved with outer membrane fusion.

Another important function of CL involves its role in mitochondrial quality control. At the site of oxidative phosphorylation, large amounts of reactive superoxide anions are produced as a by-product of electron transport, which can readily damage mitochondrial proteins, lipids, and DNA [44]. These damaged mitochondria lack proper function and need to be safely removed by mitochondrial-selective autophagy (mitophagy) [44]. This process is initiated by mitochondrial depolarization, which causes the translocation of CL from the IMM to the outside

of the OMM [45]. Externalized CL binds readily with light chain 3 proteins (LC3), and acts as an elimination signal for autophagosomes to locate/recognize damaged mitochondria [45].

As for type I cell death, CL is important for the initiation of the extrinsic apoptosis pathway [46]. CL plays a role in this death pathway by mediating the activation of caspase 8, as well as the translocation of truncated BID (t-BID) from the cytosol to the OMM [46, 47]. Both events are critical for the downstream induction of mitochondrial outer membrane permeabilization (MOMP) and the release of cytochrome c [48], such that cells with a genetic defect causing significantly reduced CL content have an impaired ability to undergo extrinsic apoptosis (Gonzalvez and colleagues (2008)). Finally, the intrinsic apoptosis pathway seems to require CL as well. CL binding to the protein BAX is critical in promoting its dimerization and activation [49]. Without the presence of CL, BAX dimers assemble into inactive oligomers and lack the ability to form stable pores in the outer mitochondrial membrane [49]. As a result, proapoptotic proteins such as Cytochrome C, Smac, and Diablo, cannot be released into the cytosol to promote downstream caspase activation. To further confirm the importance of CL in the initiation of apoptosis, I found that cardiolipin-deficient BTHS lymphoblasts had a roughly ~3 fold decrease in the relative levels of cleaved caspase 7 and ~10 fold decrease in the levels of cleaved PARP when compared to healthy lymphoblast with normal CL levels (Appendix Fig.5).

Cardiolipin Biosynthesis/remodeling

The mammalian biosynthesis of CL in the CDP-diacylglycerol pathway has been reviewed previously [50]. First, glycerol-3-phosphate (G3P) is acylated at the sn-1 position by a member of the GPAT family to form lysophosphatidic acid (lysoPA) [50]. Next lysoPA is acylated once more at the sn-2 position by a member of the AGPAT family to generate

phosphatidic acid (PA) [50]. Once inside the IMM, the condensation between PA and cytidine triphosphate creates the high energy intermediate cytidine diphosphate diacylglycerol (CDP-DAG), catalyzed by the mitochondrial enzyme CDS [50]. Subsequently, the enzyme PGP synthase (PGPS) transfers the activated phosphatidyl group from CDP-DAG onto the sn-1 position of glycerol-3-phosphate, yielding phosphatidylglycerol phosphate (PGP), which is considered the committed step of cardiolipin biosynthesis [17, 50]. After the formation of PGP, it is further de-phosphorylated by the enzyme PTPMT1 to yield phosphatidylglycerol (PG) [50]. Finally, cardiolipin synthase catalyzes the final reaction in which the precursor molecules PG and CDP-DAG are used to generate the mitochondrial glycerophospholipid, CL [50].

Analysis of different mammalian tissues has identified very specific CL fatty acyl profiles. For instance, cardiac CL has a specific fatty acyl profile that is typically close to 80% linoleic acid (18:2 n-6), with the remaining fatty acyl chains comprised of oleic acid (18:1 n-9), and stearic acid (18:0) [51]. In contrast, lymphoblast CL has an entirely different fatty acyl profile, consisting primarily of vaccenic acid (18:1 n-7), oleic acid (18:1n-9), and palmitoleic acid (16:1 n-7) [52]. These differences are mainly attributed to remodeling pathways that are active after CL is initially formed, since cardiolipin synthase lacks enzyme specificity and is unable to modify the fatty acyl composition of its substrates [53]. Therefore, CL generated through the *de novo* pathway by CLS contains the same fatty acyl composition as its precursors in CDP-DAG and PG [53]. This “immature” form of CL needs to be further remodelled in the Land’s Pathway, to create the tissue-specific fatty acyl profile necessary for proper mitochondrial function according to tissue-specific demands [54]. This process is initiated through the coordinated action of phospholipase A enzymes (PLA1 or PLA2), which deacylate fatty acyl groups from “immature” cardiolipin to produce monolysocardiolipin or

dilysocardiolipin, which is then re-acylated to the mature and functional form by remodelling enzymes [54]. These enzymes include monolysocardiolipin acyltransferase 1 (MLCL AT-1), acyl-CoA:lysocardiolipin acyltransferase (ALCAT1), and Tafazzin [54]. Tafazzin is a mitochondria-exclusive enzyme that acts predominantly as a linoleoyl transacylase, which deacylates linoleoyl residues from PC, and reesterifies them onto monolysocardiolipin, generating linoleate-enriched CL [55].

Characterisation of BTHS and healthy cell fatty acyl composition

Michael Schlame's research group has previously studied the CL acyl profile of lymphoblast cell lines derived from boys with BTHS and compared these to lymphoblast lines obtained from healthy age, sex, and ethnicity matched controls. The four most abundant fatty acyl species within CL of healthy lymphoblast are vaccenic acid (18:1n-7), oleic acid (18:1n-9), palmitoleic acid (16:1n-7), and linoleic acid (18:2n-6). Vaccenic acid (18:1n-7) is a monounsaturated fatty acid found in ruminant animals, human breast milk and dairy products [56, 57]. While it is possible to synthesize 18:1n-7 through the elongation of palmitoleic acid with ELOVL6 [58], a diet enriched with 9.1g of 18:1n-7 led to a 1900% increase in the concentration of 18:1n-7 in the phospholipid fractions of the mesenteric lymph nodes of rats [59]. This suggest that the primary source of 18:1n-7 in immune cells likely comes from direct dietary consumptions. Additionally, the observed increase in 18:1n-7 is also associated with a decrease in the number of splenocytes, helper T-cells, and inflammatory markers (IL-2, IL-10, and TNF α), suggesting that its relative abundance in phospholipids can be a factor in the regulation of immune cell number and immune function [59].

Oleic acid (18:1n-9) is another monounsaturated fatty acid found in high abundance in sunflower oil and olive oil [60, 61]. Other than its direct dietary source, it is also synthesized *de novo* in humans, from the desaturation of stearic acid (18:0) using delta 9 desaturase [62]. Recently, it was suggested that 18:1n-9 is the most efficient fatty acid that is incorporated into CL, since it does not require further elongation or desaturation prior to acylation [63]. Hence, 18:1n-9 is highly abundant within immune cells, accounting for up to 22% of the total fatty acids in human lymphoblast CL [52]. Furthermore, 18:1n-9 also seems to be important for immune function as well, as a decrease in 18:1n-9 in the phospholipid fraction of spleen lymphocytes, caused an overall decrease in lymphocyte proliferative rate and lymphocyte activation [64].

Palmitoleic acid (16:1n-7) is the third most abundant fatty acyl within CL, accounting for ~16% of the total fatty acyl species [52]. The primary source of 16:1n-7 in humans, involves the biosynthesis from palmitic acid (16:0), by delta-9-desaturase, or by direct uptake from dietary sources such as macadamia oil, salmon, and ruminant fat [65]. While, a majority of studies on 16:1n-7 focused on its effects in metabolic diseases such as obesity and diabetes, 16:1n-7 is also involved in immune cell proliferation as well [66], such that an increase in its incorporation within CL is highly correlated with an increase in T-lymphocyte proliferation [66].

Linoleic acid (18:2n-6) is a polyunsaturated fatty acid found in vegetable oils, nuts, seeds, meats, and eggs [67]. As it is an essential fatty acid, humans cannot directly produce 18:2n-6 from *de novo* synthesis [67]. Therefore, the only source of 18:2n-6 in immune cells comes from its direct dietary consumptions. Despite this, 18:2n-6 was still reported to be highly abundant in the CL of human lymphoblasts, accounting for up to 12.3% of the total fatty acyl species [52]. Since the relative levels of tetra-linoleyl cardiolipin was previously shown to be highly

associated with the proliferation rate of healthy T lymphoblast [66], 18:2n-6 seems to play an important role in the regulation of immune cell number.

When comparing between the CL fatty acyl profile of healthy and BTHS lymphoblasts, differences can be observed in oleic acid (18:1n-9) palmitoleic acid (16:1n-9), and linoleic acid levels (18:2n-6), which were significantly lower in CL from BTHS lymphoblasts compared to healthy control lymphoblasts (18:1n-9 [healthy ~21.8 vs BTHS ~10%], 16:1n-9 [healthy ~15.5% vs BTHS ~5.4%], 18:2n-6 [healthy ~12.3 vs BTHS ~1.4%]). In contrast, vaccenic acid levels (18:1n-7) were significantly higher in the CL of BTHS lymphoblast, which became the most prominent fatty acyl species (18:1n-7 [healthy ~37.0 vs BTHS ~55.5%]) [52]. Furthermore, BTHS also caused a general shift from a CL profile that was predominantly enriched in unsaturated fatty acyl chains such as palmitoleic (16:1 n-9) and linoleic acid (18:2 n-6), to a profile that was highly saturated, with palmitic (16:0) and stearic acid (18:0) species (**Table 1**) [52].

Table 1: Relative fatty acyl composition of lymphoblast cardiolipin

Fatty acid	Control	BTHS
<i>14:0</i>	1.8 ± 0.3	2.5 ± 0.2
<i>16:0</i>	6.1 ± 0.7	19.5 ± 0.4*
<i>16:1</i>	15.5 ± 0.9	5.4 ± 1.0*
<i>18:0</i>	1.5 ± 0.1	5.7 ± 0.1*
<i>18:1 n-9</i>	21.8 ± 4.3	10.0 ± 1.1*
<i>18:1 n-7</i>	37.0 ± 3.0	55.5 ± 1.1*
<i>18:2</i>	12.3 ± 1.0	1.4 ± 0.4*
<i>20:3</i>	3.9 ± 0.4	0.1 ± 0.1*

Table adapted from Xu et al. (2005). Relative fatty acyl species composition are expressed as mass%. *P>0.05 versus Control.

Differences between BTHS and healthy lymphoblast in mitochondrial function and ultrastructure

Additional work from Schlame's research group determined that the mitochondrial membrane potential was also significantly affected in BTHS, which caused a decrease in oxidative phosphorylation capacity [52]. Interestingly, however, the total rate of ATP production did not change between the two groups, due to the hyperproliferation of mitochondria in BTHS lymphoblasts, which compensated [52]. Following this study, electron micrographs were taken of both BTHS and healthy lymphoblasts, and their mitochondrial ultrastructure was examined in detail [68]. As expected, mitochondria from control lymphoblasts exhibited parallel cristae structure, which connected to the inner boundary membrane and extended towards the middle of the organelle as tubular structures [68]. Lymphoblasts from BTHS subjects, however, showed a

lack of proper alignment of cristae, which was collapsed to the periphery of the mitochondria [68]. Additionally, these cristae lack intracristae spaces, due to the close adhesion between the two sides of the crista membrane [68]. As a result, giant/swollen mitochondria were apparent, which had a “honeycomb like appearance (Fig. 2) [68].

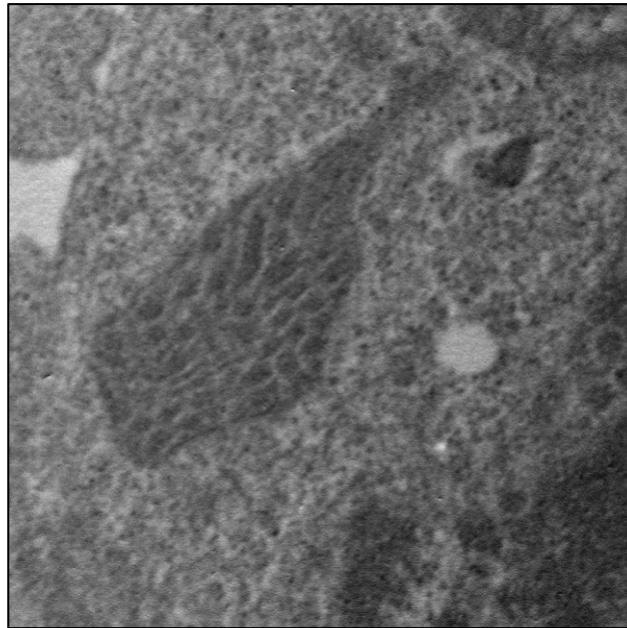


Figure 2: Cross-sectional view of a lymphoblast mitochondria derived from a 10-year old male Barth patient. In preliminary electron microscopy studies using B-lymphoblasts from a patient with Barth Syndrome, giant/swollen mitochondria with a characteristic “honeycomb like appearance” were observed.

Therapeutic strategies using N-acylethanolamines (NAEs)

N-acylethanolamines (NAEs) are a group of endogenously synthesized bioactive lipids comprised of a fatty acyl chain that is attached onto an ethanolamine group [69]. Their effects on biological processes include, but are not limited to, nociception, appetite suppression, hypothermia and pro- and anti-inflammation regulation [70-72]. Different NAE have different actions on the body. For example, anandamide (AEA) is best known for its effects on the central nervous system to regulate mood [73], analgesia [71], appetite [74], and the dopamine reward system [75], modulated through the agonism of G-protein-coupled receptor CB1 and CB2, the peroxisomal proliferator-activated receptors (PPAR α & PPAR γ), and the transient receptor potential vanilloid type-1 (TRPV1) [71, 73-76]. OEA on the other hand, is an anorexic agent known to reduce feeding activity in animal models, mediated by the binding of receptors PPAR α , TRPV1, and GPR119 [71, 77, 78]. Unlike AEA, OEA has no affinity towards the cannabinoid receptor CB1 and CB2, which means that the direct administration of OEA is unlikely to induce any psychoactive effects [77]. Finally, LEA is perhaps one of the least studied NAE. Its known actions include the modulation of inflammation and food intake in animal models, through the induction of CB2, TRPV1, and PPAR α [79-81]. Since LEA also binds weakly to CB1 receptor [82], it is suggested that LEA administration should elicit minor psychoactive effects similar to AEA. Since LEA has activity with TRPV1 and PPAR α , like OEA, we also examined this NAE.

The endogenous generation of NAE involves a two-step reaction, which produces N-acylphosphatidylethanolamine (NAPE) through the transfer of an *sn-1* acyl chain from a glycerophospholipid onto the amino group of phosphatidylethanolamine (PE), catalyzed by calcium-dependent N-acyltransferase (NAT) [71]. Next, a molecule of phosphatidic acid (PA) is

hydrolyzed from NAPE by the enzyme NAPE-phospholipase D (NAPE-PLD), generating the bioactive lipid NAE [71]. In an alternative pathway without the use of NAPE-PLD, a group of Ib secretory PLA2 (sPLA2) hydrolyzes a fatty acyl group from NAPE, creating lysoNAPE [83], which is further hydrolyzed by an enzyme lyso-PLD to generate NAE [83]. Quantitatively, the major NAE species synthesized within mammalian cells are stearoylethanolamide (SEA), oleoylethanolamide (OEA), palmitoylethanolamide (PEA), and linoleoylethanolamide (LEA) [71, 84].

Identification of novel therapeutic agents to improve CL profiles and mitochondrial function in patients with BTHS could have significant benefit in reducing morbidity and mortality. In prior work by the Duncan Lab, it was determined that treatment of a BTHS lymphoblast cell line with oleoylethanolamide (OEA) partially rescued the number of cells per flask when cells were cultured over 3 days [85]. Given these promising preliminary data, further studies on OEA, as well as another NAE, linoleoylethanolamide (LEA), were planned. OEA and LEA were the chosen candidate, as two of their downstream receptors (i.e. PPAR α and TRPV1) have been previously shown to regulate phospholipid metabolism [86-88]. Specifically, the knockout of PPAR α in *PPAR α ^{-/-}* mice, lead to a significant reduction in the total phospholipid content of hepatic tissues by nearly 45% [87]. Furthermore, the activation of PPAR α also resulted in an increase in the biosynthesis of CL both *in vivo* and *in vitro*, through the induction of *PGPS*, *CDS1*, and *CDS2* [89]. Taken together, this suggests that OEA, as a PPAR α agonist, may also act similarly to increase CL levels. As for TRPV1, its activation has been noted to promoted the synthesis of phosphatidylinositol phosphates (PIPs) from the precursor phosphatidylinositol (PI) [86]. Therefore, it is possible that the treatment with OEA or LEA may have a beneficial effect on the function of BTHS lymphoblast, potentially through the direct

modulation of the metabolism of CL. In addition, LEA was also shown previously to regulate the inflammatory response of immune cells, through the activations of CB2. Since numerous NAEs (PEA, 2-AG, DEA, DHEA & AEA) act through the same CB2 receptor [90, 91], the effects of LEA on BTHS lymphoblast may provide an important insight on the efficacy of NAEs, as therapeutic modulators of BTHS.

Chapter Three: Thesis Study I – Effects of OEA and LEA on BTHS and control lymphoblast cell number

Introduction and Study Rationale

Barth Syndrome (BTHS) is a rare X-linked disorder caused by mutations in the *TAZ* gene that encodes for the enzyme Tafazzin [92]. Normally, Tafazzin participates in the remodelling of nascent cardiolipin, through the coordinated action of phospholipase A enzymes that produce monolysocardiolipin, which is then reesterified into mature cardiolipin enriched with linoleate [55, 92]. In the case of BTHS, mutations impair the function of the Tafazzin enzyme, and decreases the enzyme's ability to remodel cardiolipin [4, 92]. This causes an accumulation of the intermediate product monolysocardiolipin (MLCL), a subsequent decrease in total CL levels, and significant alterations in CL fatty acyl composition [4, 52]. Due to the many important roles CL plays in the mitochondria, such as oxidative phosphorylation, cristae organization, mitochondrial dynamics and quality control [19, 28, 93, 94], a decrease in CL levels and a change in its fatty acyl composition, have been linked to the impairment of critical mitochondrial functions, leading to a wide variety of disorders [7].

One of the major disorder of BTHS is cyclic neutropenia, which is caused by abnormally low concentrations of circulating neutrophils in the blood, leading to increased susceptibility to sepsis from infections [7]. Indeed, nearly half of the patients in the original characterization study by Barth et al (1983) [2], died of bacterial sepsis rather than from complications of cardiomyopathy. Hence, the discovery of treatment strategies that may lead to improved BTHS immunity are essential to the overall survival of BTHS patients and should be a major therapeutic focus. Recently, in a 2020 BSF Scientific and Medical Symposium, unpublished findings from a group of researchers discovered a deficiency in total lymphocyte count in a

Tafazzin-deficient mouse model [13]. This suggest that the immune deficiencies in BTHS might not be limited to neutropenia and could also manifest into lymphopenia as well. Due to the rarity of this disease, lymphocyte sample collections from BTHS patients are scarce. Therefore, a precursor cell (lymphoblast) will be used in place of lymphocyte as the study model, due to its ease of access [95].

Lymphoblasts derived from BTHS patients exhibit abnormal CL metabolism, CL deficiency, and altered CL composition, leading to decreased membrane potential, increased ROS production, and abnormal mitochondrial ultrastructure [52, 96]. Although BTHS lymphoblasts are well characterized in the literature [46, 52, 68, 96], little is yet known regarding the effects of BTHS on lymphoblast growth both *in vivo* and *in vitro*. Whether, the observed deficit in cell function associated with BTHS, leads to an overall decrease in lymphoblast number, still needs to be elucidated. Based on this, a former PhD student at the Duncan lab cultured one set of BTHS and healthy lymphoblasts, and determined that BTHS lymphoblasts exhibited impairments in growth, as evident by the decrease in cell number by 42% relative to healthy [85]. In the same study, the treatment using 1uM of OEA had a partial effect to increase the number of BTHS lymphoblasts, so that the differences between BTHS and healthy cell number was no longer as prominent [85]. OEA acts through the receptors PPAR α and TRPV1, which have both been shown previously to regulate phospholipid metabolism [86, 87, 89]. Therefore, it is possible that the effects of OEA on BTHS lymphoblast growth might be associated with its ability to alter CL metabolism. Nonetheless, the novel therapeutic role of OEA in the previous work, was only shown in one set of BTHS and healthy cell lines [85]. Seeing that the severity and prognosis of Barth syndrome can vary greatly depending on the

types of mutations in the Tafazzin gene [97], additional BTHS and healthy lymphoblast cell lines will need to be tested, in order to further establish the therapeutic potential of OEA.

OEA belongs to a large group of NAEs, which are all known bioactive lipids capable of binding to multiple receptors, causing many downstream effects [71]. OEA is different compared to many other NAEs, since it does not have actions on the CB1 and CB2 receptor [77]. Since the CB2 receptor has previously been shown to modulate the inflammatory response of immune cells [98], LEA, an agonist to CB1 and CB2 as well as PPAR α and TRPV1, will also be assessed as a potential therapeutic modulator of BTHS lymphoblasts. In summary, the overarching objective of this chapter was to assess the effects of OEA and LEA on BTH and healthy lymphoblast cell numbers.

Objectives and Hypothesis

Objective: To investigate effects of OEA or LEA treatment for 96 hours on the number of cultured BTHS lymphoblasts, relative to the same cells treated with vehicle alone (control), and relative to treated or untreated healthy matched control lymphoblast cell lines.

Hypothesis: Treatment for 96-hours using OEA or LEA will significantly increase the number of cultured BTHS lymphoblasts relative to the number of BTHS lymphoblast cells present in flasks treated with vehicle alone. The numbers of BTHS lymphoblasts in treated flasks will increase to a level that is lower than the number of healthy matched control cells, indicating only a partial rescue. There will be no difference in cell numbers between treated and untreated healthy control lymphoblasts.

Method:

NAE treatment and Cell counting:

Epstein-Bar virus-transformed lymphoblasts from 10 males aged 10 and under, with or without Barth syndrome (BTHS) were obtained from Coriell Biorepository (Individual BTHS and healthy donor characteristics described in **table 2**) [15]. Lymphoblasts from both BTHS and healthy donors were seeded in 25cm² culture flasks, at an initial seeding density of 1.2 million cells. Cells were cultured in Roswell Park Memorial Institute (RPMI-1640) media with 10% charcoal-stripped FBS, 1% penicillin-streptomycin, and treated with either OEA or LEA at a final concentration of 1uM, or 0.1% vehicle (ETOH) and growth was maintained at 37°C in 5% CO₂ for a total of 4 days (96 hours). On day 0, baseline cell numbers were measured for each BTHS and healthy group to ensure accurate seeding density. Next, total cell number were recorded after every 24 hours, for a total of 4 time points (96 hours). To perform the cell counts, each treatment flasks were gently mixed by pipetting up and down using a 10 mL serological pipet. Next, a 10 uL volume from each treatment flask was aliquoted and mixed with 30 uL of RMPI media to make a dilution factor of 1/4. Finally, a 10 uL volume from the diluted sample was added to both sides of the hemocytometer, where the cells were manually counted following the instructions provided by ThermoFisher Scientific [99].

For the completion of this experiment, BTHS and healthy lymphoblast from 5 distinct donors were used for the study of OEA, and four distinct donors for the study of LEA. All lines were counted either in triplicate or duplicate, and these technical replicates were averaged to obtain single biological measures at each time point.

Statistical Analysis:

Data are expressed as means \pm S.E.M, or as individual values. Repeated measures two-way analysis of variance (ANOVA) with multiple comparisons using Sidak's post-hoc test was used to analyze for the effects of treatments within cell types, and effects of cell type within each treatment. In addition, interactions between cell types and treatments were assessed using a two-way analysis of variance (ANOVA) with Tukey's multiple comparisons post-hoc test.

Differences between treated and untreated cells for individuals were assessed by Student's paired t-test. Significant differences were accepted at $P < 0.05$.

Table 2: Individual Barth and healthy donor characteristics from Coriell Biorepository

Order number	Sex	Age	Type of mutation
GM22192	Male	10 years	C>T change in exon 3 of TAZ (G4.5) gene. Resulting in substitution of cysteine for arginine at codon 94 [Arg94Cys (R94C)]
GM22194	Male	9 years	Complete deletion of TAZ (G4.5) gene
GM22193	Male	10 years	T>A change in exon 6 of TAZ (G4.5) gene. Result in premature stop codon [Leu166Ter (L166X)]
GM22150	Male	7 years	G>A change in exon 2 of the TAZ (G4.5) gene. Result in stop codon [Trp79Ter (W79X)]
GM22163	Male	9 years	1 bp deletion (171delA) in exon 2. Result in a frameshift after amino acid 57 [Gly58AlafsX25]
AG15022	Male	10 years	Apparently healthy individual
AG14731	Male	8 years	Apparently healthy individual
AG14948	Male	10 years	Apparently healthy individual
AG14750	Male	9 years	Apparently healthy individual
AG14947	Male	10 years	Apparently healthy individual

Results

OEA treatment of BTHS lymphoblast partially restored the deficit in total cell number. No significant effects were observed with LEA treatment. Following the first 24 hours of growth, no significant differences in cell number were observed between healthy and BTHS lymphoblasts. Growth impairments in BTHS lines were only apparent after the 72nd hour, in which the mean BTH lymphoblast number (~3.0 million) was significantly different compared to the mean healthy lymphoblast number (~4.4 million). OEA partially rescued the deficit in BTHS cell number observed on the 72nd hour, by increasing the total cell number to 3.4 million. By the 96th hour, the differences in total cell number between OEA-treated BTHS lymphoblasts and healthy lymphoblasts was no longer significantly different (**Fig. 3**). LEA on the other hand had little effect, since it did not significantly change BTH lymphoblast number in any of the 4 timepoints (**Fig. 3**).

Following the 4-day growth analysis, area under the curve (AUC) analysis were also used to help represent the effects of LEA and OEA on BTHS and healthy lymphoblast cell number. First, there was a statistically significant difference in the AUC of vehicle-treated healthy lymphoblasts & BTHS lymphoblasts counted for up to four days ($P < 0.01$) (**Fig. 3**). Treatment with OEA had a partial effect to increase the AUC of the BTHS lymphoblast mean cell count, so that the AUC was significantly different than the AUC of untreated BTHS lymphoblasts ($P < 0.01$), but was still significantly different compared to the healthy vehicle group ($P > 0.05$) (**Fig. 3**). LEA had only a minor effect on the AUC that did not reach statistical significance as a group effect (**Fig. 3**).

All BTH lymphoblast donors responded to OEA treatment. LEA had a minor effect to increase cell number in three out of the four BTH donors. While the group analysis

method gives insight on the effects of OEA and LEA on the mean cell number of all sampled BTHS and healthy lymphoblasts, it does little to capture the individual responses to OEA and LEA treatment. Each lymphoblast line represents a distinct human donor, with some differences in characteristics, including cell proliferative capacity. After equal seeding on Day 1, total cell number on Day 4 could vary by up to 1.3×10^6 cells between individual healthy lines, and by up to 1.6×10^6 cells between individual BTHS lymphoblast lines (**Appendix Figs. 1 & 2**). Thus, analysis of individual responses is important to illustrate clinically significant effects (**Figs. 4 & 5**). Total cell number was lower on day 4 in four out of five healthy lymphoblast lines treated with OEA, and in three out of four healthy lymphoblast lines treated with LEA, although this did not reach significance (**Figs. 4a & 5a**). In contrast to healthy lymphoblasts, OEA treatment resulted in a higher total cell number on day 4 for all five BTHS lymphoblast lines ($P < 0.05$) (**Fig. 4b**). LEA treatment slightly increased total cell number in three out of four BTHS lymphoblast lines, however, this did not reach statistical significance (**Fig. 5b**). The relative difference in response to OEA and LEA between healthy donor lines and Barth Syndrome donor lines is illustrated in Figures 4C and 5C. Healthy cell lines treated with OEA or LEA had, on average, fewer cells than untreated matched lines on day 4, whereas cell lines from Barth Syndrome patients had more. The difference between these responses was statistically significant ($P < 0.01$).

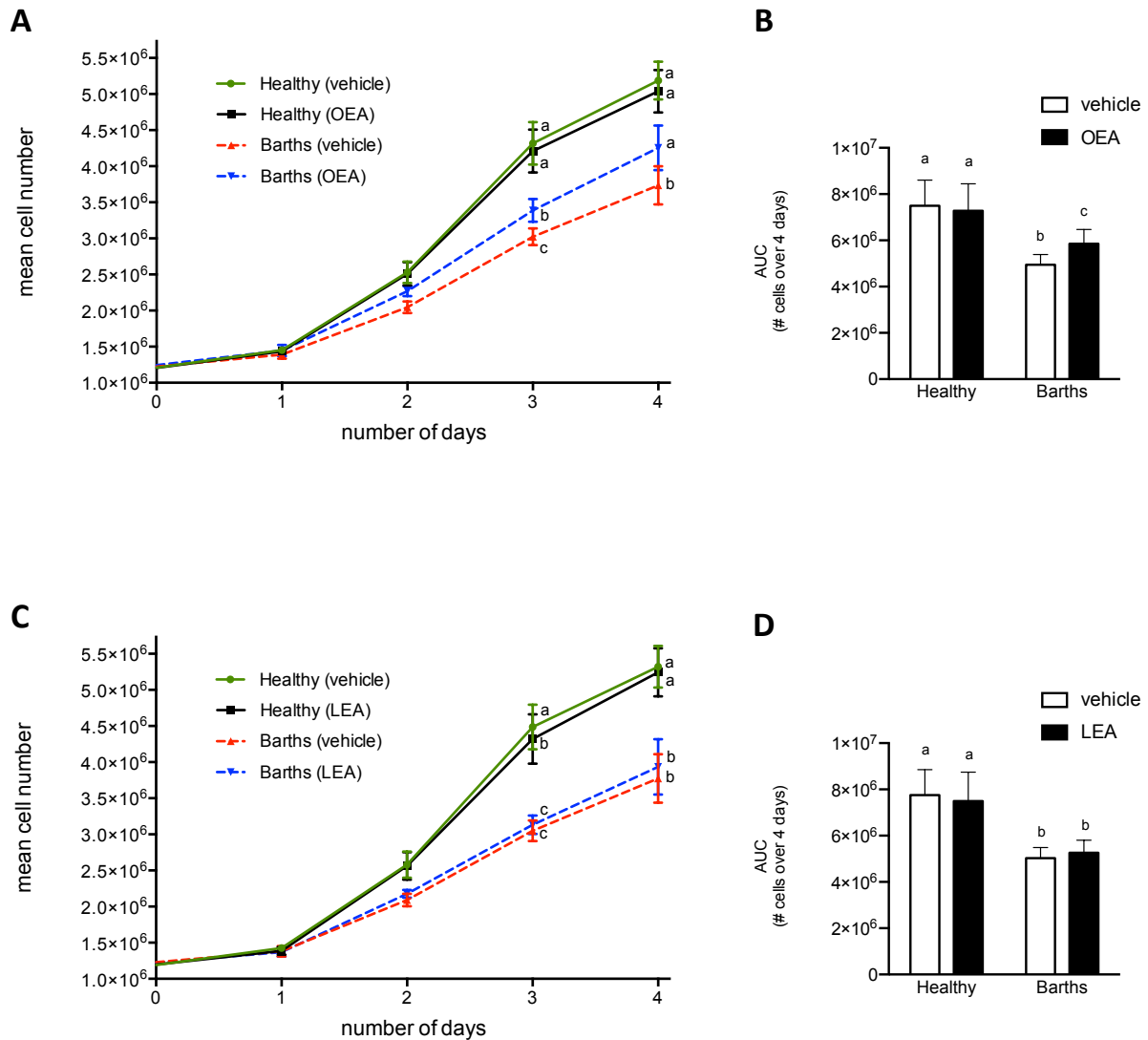


Figure 3: Effect of OEA and LEA on lymphoblast cell number over 4 days of growth.

Lymphoblasts from donors with BTHS, or healthy matched controls, were treated with vehicle control (0.1% v/v ethanol) or either (A) 1 μ M OEA (n=5, biological rep) or (C) 1 μ M LEA (n=4, biological rep). Group values are shown. (B,D) The right panel shows the area under the curve (AUC) of the mean cell number over 4 days (B, n=5), (D, n=4). Data are means \pm S.E.M.

^{abc}Symbols with a different letter are significantly different, $P < 0.05$. Repeated measures two-way ANOVA with was used to analyze for effects of treatments within cell types, and effects of cell types within treatments, with Sidak's multiple comparisons test. Two-way ANOVA with Tukey's multiple comparisons test was further used to analyze for interactions between cell types and treatments. * $P < 0.05$, ** $P < 0.01$, one-way ANOVA with Tukey's post-hoc analysis.

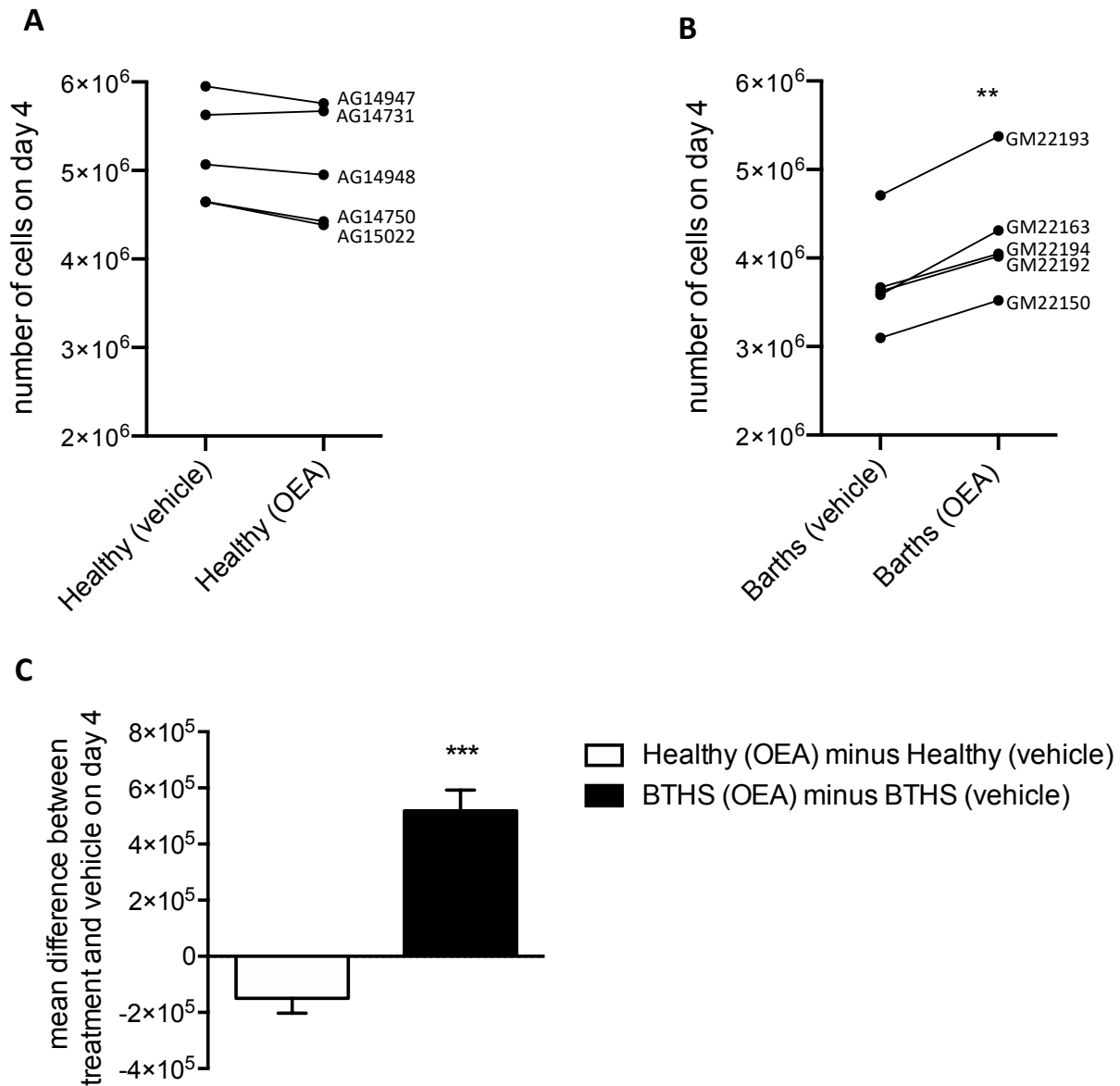


Figure 4: Individual donor responses to the effect of OEA treatment for 4 days on cell number. (A) In the cell lines derived from healthy donors, four of five lines treated with OEA had lower cell numbers at day four than when treated with vehicle, indicating a slight negative effect that did not reach significance. (B) In the cell lines derived from donors with Barth Syndrome, all five lines treated with OEA had a positive response to treatment versus vehicle alone, which was statistically significant. (C) The mean response of healthy donor cells versus the response of cells from donors with Barth Syndrome to treatment with OEA is illustrated. In the healthy cell lines, treatment with OEA resulted in almost 2×10^5 fewer cells by day 4 than was evident when only vehicle was used. In cell lines from donors with Barth Syndrome, however, there were approximately 5×10^5 more cells on day four when OEA treatment was used ($n=5$, biological replicates). Data in A and B were analyzed by paired Students t-test, and Data in C were analyzed by Student's unpaired t-test * $P < 0.05$, *** $P < 0.001$

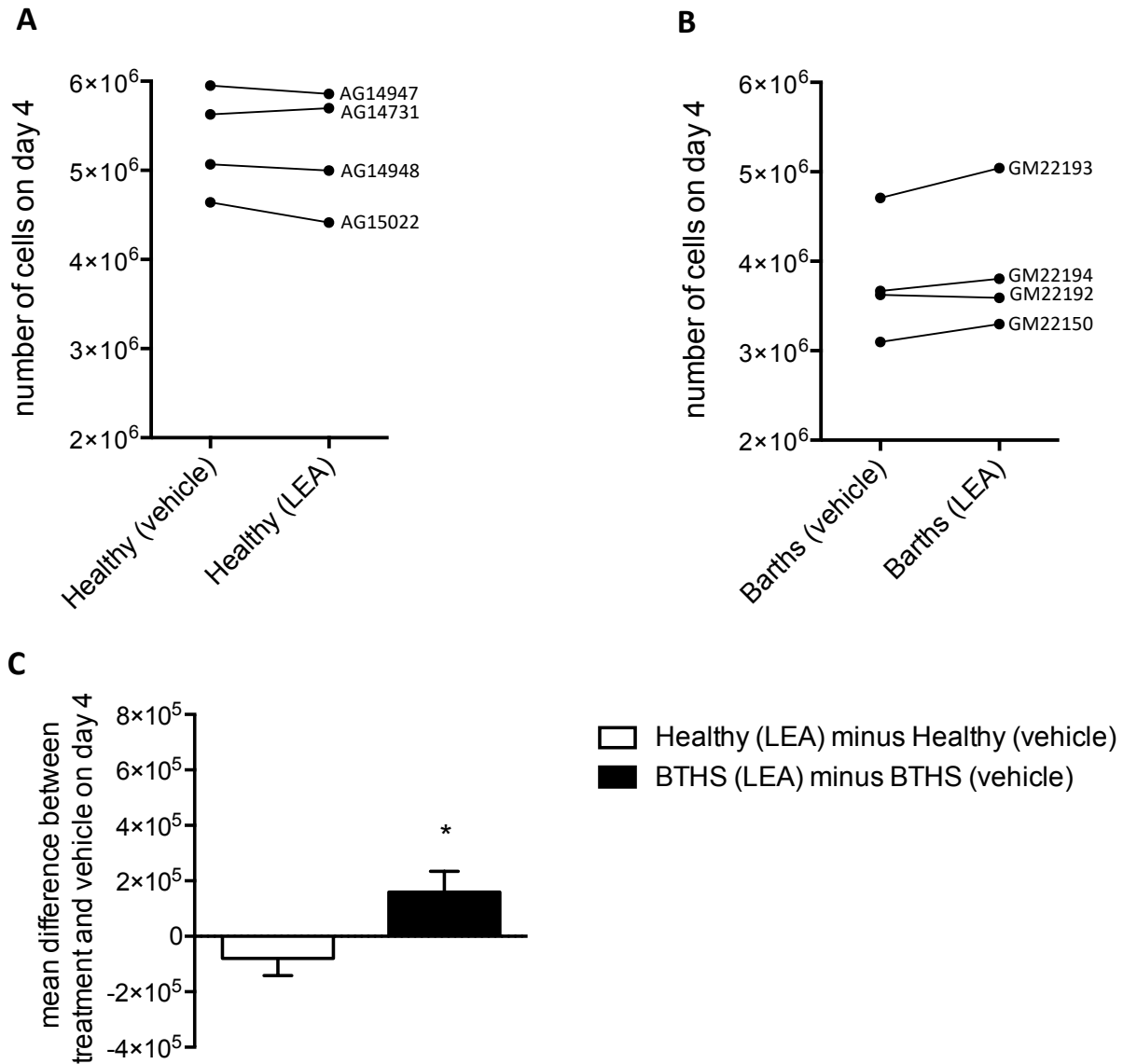


Figure 5: Individual donor responses to the effect of LEA treatment for 4 days on cell number. (A) In the cell lines derived from healthy donors, three of four lines treated with LEA had lower cell numbers at day four than when treated with vehicle, indicating a slight negative effect that did not reach significance. (B) In the cell lines derived from donors with Barth Syndrome, three of four lines treated with LEA had a slight positive response to treatment versus vehicle alone, which also did not reach significance. (C) The relative response of healthy donor cells versus the response of cells from donors with Barth Syndrome to treatment with LEA is illustrated. In the healthy cell lines, treatment with LEA resulted in almost 1×10^5 fewer cells by day 4 than was evident when only vehicle was used. In cell lines from donors with Barth Syndrome, there were almost 2×10^5 more cells on day four when LEA treatment was used. (n=4, biological replicates). Data in A and B were analyzed by paired Students t-test, and Data in C were analyzed by Student's unpaired t-test *P<0.05

Discussion

The current study examined the effects of treatment with two NAEs (i.e. OEA and LEA) on BTHS and healthy lymphoblast cell number. While preliminary data from the Duncan lab have previously shown an effect of OEA to increase the observed deficit in cell number of one line of BTHS lymphoblast [85], no further work since then had been performed to determine the effects of OEA on additional cell lines. Given that the symptoms and severity of BTHS can vary between each individual patient, it is thus important to establish the effects of OEA in a larger cohort of BTHS patients [97]. This work, for the first time, demonstrated that the treatment with OEA lead to an increase in the mean cell number of five BTHS lymphoblast cell lines, such that it was no longer significantly different from the number of treated or untreated healthy controls, by the 4th day of growth. Perhaps more astonishing, is that all five out of the five tested BTHS donors had a positive response to OEA, and their relative increase in total cell number by day four was rather consistent between each donor. Thus, OEA presents as a potential promising therapeutic agent for Barth Syndrome, and its effects on cell number may help to ameliorate immune deficiencies as observed in lymphopenia.

Another major objective of this thesis chapter was to examine the effects of an additional NAE on BTHS and healthy lymphoblast number. LEA was the chosen candidate, as it was previously shown to act on both PPAR α and TRPV1 [79, 81]. This suggest that LEA may have a role in the modulation of cardiolipin metabolism. In addition, LEA also had an effect to modulate the inflammatory response of immune cells, through the cannabinoid receptor CB2 [80]. Since the CB2 receptor is highly expressed in many immune cell types, and its activation has been found to modulate immune cell development, migration, proliferation, and function [98], I hypothesized that the treatment with LEA will increase the total cell number of BTHS

lymphoblasts, mediated by an increase in the rate of lymphoblast proliferation and a restoration of the CL content. Despite these speculations, results from my study indicated otherwise, and the treatment with LEA did not result in any significant changes in the average BTHS cell number of four distinct donors. Since LEA did not increase the number of lymphoblasts, this lack of an effect suggested that LEA should not be considered as a therapeutic treatment option for BTHS patients with lymphopenia. Moving forward, OEA will be the primary focus of this study, due to its promising effects on BTHS lymphoblast number.

While the significant detriment in total cell number of BTHS lymphoblasts was observed here in this study, little is still known as to what is causing this dramatic deficit. To speculate, it is likely that the growth impairments observed in BTHS were caused by decreased CL content and altered CL composition, leading to either decreased cell proliferation and/or increased cell death. One of the main differences in the CL fatty acyl profile between BTHS and healthy lymphoblast involves the lower relative levels of 18:1n-9, 16:1n-7, and 18:2n-6, which were shifted primarily into higher 18:1n-7 levels [52]. Since these fatty acids have been previously reported to be important regulators of lymphocyte proliferation [59, 64, 66], alternations to their relative content might be a contributing factor to an overall decrease in BTHS lymphoblast proliferative capacity. Additionally, decreased CL content and altered CL composition has also been demonstrated to impair electron transport chain function, causing decreased mitochondrial membrane potential [52]. This can directly increase the production of ROS, which would normal lead to increased cell death mediated by apoptosis. Since BTHS cells have impaired ability to initiate apoptosis due to the blocking of the pathway at the levels of t-BID and BAX, BTHS lymphoblast cell death will instead be mediated by other death pathways, such as necroptosis or autophagic cell death [100, 101]. Consequently, the combined effects of impaired lymphoblast

proliferation and increased cell death are two of the most likely causes of the observed differences in cell number between BTHS and healthy lymphoblasts.

As for the effects of OEA on BTHS, a likely potential mechanism behind the effects of OEA to increase lymphoblast cell number could be postulated to be the activation of TRPV1 and PPAR α . Both receptors, to an extent, have been shown to regulate phospholipid metabolism, such that the activation of PPAR α directly increases the biosynthesis of CL in cardiac tissues [89]. In theory, an increase in the CL content of BTHS cells with CL deficiency should improve mitochondrial energy production necessary to keep up with high energy demands during cellular proliferation. Alternatively, increased CL content may also restore the mitochondrial membrane potential of BTHS lymphoblasts, which would lead to decreased ROS production and lymphoblast death. To validate these proposed theories, additional studies are needed to confirm the effects of OEA on cardiolipin metabolism of BTHS lymphoblasts.

Chapter Four: Thesis Study II – Effects of OEA on CL metabolism and composition

Study Rationale

In thesis study I, I monitored the effects of treatment with two NAEs on BTHS and healthy lymphoblast growth over four days. Treatment with OEA partially rescued the deficit in mean cell number of BTHS lymphoblast, such that all tested donors responded positively to treatment. LEA on the other hand, had minor effects, and only slightly increased the cell number in three out of four tested donors, which was not significant. Based on these results, OEA was believed to be more promising as a therapeutic modulator of BTHS, and became the primary focus of this thesis.

Although extensive evidence was provided that confirmed the positive effects of OEA on BTHS lymphoblast growth, the direct mechanism to explain how OEA is eliciting this effect was still unclear. Prior works to characterize lymphoblasts from BTHS patients reported significant declines in CL levels, in-conjunction with major alternations in the CL fatty acyl profile [52, 96]. Considering that the presence of CL is vital for mitochondrial health, and proper function of the mitochondria is necessary for cell proliferation and maintaining overall cell survival [94, 102], it is possible that the effects of OEA to increase BTHS lymphoblast growth was caused by the direct increase in endogenous CL biosynthesis, mediated by the activation of TRPV1 and PPAR α receptors involved in regulating genes involved in phospholipid metabolism.

Prior work by our laboratory in a single Barth and single control cell line has demonstrated significantly higher expression of *CDS1* and *GPAT3*, in the BTHS line [85]. Notably, this difference was largely abrogated when cells were treated with 1 μ M OEA [85]. Whether similar differences in the expression of cardiolipin biosynthetic genes occurs in other

cell lines, and whether OEA similarly affects relative differences in expression, had not yet been tested. To continue this work, the overarching objective of this chapter was to assess the capacity of OEA treatment to modulate genes involved in *de novo* synthesis of CL in three BTHS and healthy cell lines. Furthermore, preliminary analysis of the effects of OEA on CL content and composition will also be elucidated in a single set of BTHS and healthy lymphoblast lines.

Objectives and Hypothesis:

Objective 1: The first objective is to analyze the expression of genes involved in cardiolipin synthesis in lymphoblast lines from boys with Barth Syndrome compared to healthy control lines, and to further determine whether this expression is altered by OEA treatment.

Hypothesis: It is expected that the expression of genes involved in the *de novo* synthesis of cardiolipin will be elevated in Barth's lymphoblast lines relative to control lines. OEA treatment for 96 hours is predicted to partially normalize this expression, reflecting the better mitochondrial health of cells.

Objective 2: To investigate if treatment with OEA can increase the total CL content in one set of BTHS lymphoblasts, to a level that is comparable to that of a healthy control.

Hypothesis: OEA treatment for 96 hours will increase the total CL content in cultured lymphoblasts derived from a BTHS patient, compared to the same cell line treated with vehicle alone, to a level that is comparable to that of the healthy age/sex matched controls. Treatment with OEA will not alter CL total content in healthy control lymphoblasts.

Objective 3: To characterize the fatty acyl composition of CL in one set of BTHS and healthy lymphoblasts, treated with either OEA or vehicle for 96 hours.

Hypothesis: Treatment with OEA for 96 hours will significantly enrich CL of BTHS lymphoblasts with oleic acid (18:1 n9) and palmitoleic acid (16:1n7) but will reduce vaccenic acid (18:1 n7). No significant changes in the relative composition of CL will be observed in the healthy control treated with OEA.

Methods:

RNA extraction, Reverse transcription, and Quantitative polymerase chain reaction:

Total RNA was isolated from cell homogenates using TRIzol Reagent (Invitrogen, Carlsbad CA) according to the manufacturer's protocol [103]. To begin, healthy and Barth lymphoblasts were treated with 1 μM of OEA or vehicle (0.1% ethanol) and grown in 25 cm^2 flasks at an initial seeding density of 1.2 million cells. Following a four-day growth period (96 h), the cells were harvested into 50 mL Falcon tubes and centrifugated at $1000 \times g$ for 5 min. The supernatant was removed, and the cell pellet was suspended in TRIzol Reagent ($\sim 0.75\text{mL}/5 \times 10^6$ cells) and mechanically disrupted by vigorous pipetting. Subsequently, the samples were incubated at room temperature for 5 min prior to the addition of chloroform (20% of TRIzol volume), where it was vigorously shaken for 15-20 s. This was followed by a 2 min incubation and centrifugation at $12,000 \times g$ for 15 min (4°C). The resulting upper-most aqueous layer was mixed with isopropanol (50% volume of TRIzol) and incubated for 10 min at room temperature. The supernatant was discarded, and the pellet was then centrifugated at $7,500 \times g$ for 5 min (4°C) in 0.75mL of 75% ethanol. After the centrifugation, ethanol was discarded from the sample, air-dried for 5 min, and 50 μL of ddH₂O was added. Finally, the samples were incubated at 55°C for 10 min to facilitate solubilization and then stored at -80°C .

Next, a high-capacity cDNA reverse transcription kit (Thermo Scientific) was used to reverse transcribe the sample RNA to cDNA, following the manufacturer's protocol [104]. Briefly, RNA samples were quantified using a Nanodrop 2000 Spectrophotometer (ThermoScientific, Waltham MA) and adjusted to a final concentration of 1 $\mu\text{g}/5 \mu\text{L}$ with ddH₂O. 2 μg of RNA was added to 10 μL of a reverse-transcription master mix with pre-added RNase inhibitors (2 μL of 10 x RT buffer, 0.8 μL of dNTP mix (100 nM), 2 μL of RT random Primers

(oligo dTs), 1 μ L of Reverse Transcriptase, 4.2 μ L of ddH₂O). Each sample was placed in the thermocycler with the following cycling conditions: 25°C for 12 min, 37°C for 120 min, and 85°C for 5 min. Lastly, each sample was diluted to give a 1:5 ratio with ddH₂O and stored at -80°C.

For the real-time polymerase chain reaction (qPCR) assays, 1 μ L of cDNA was added to a 96 well plate containing, 5 μ L SYBRTM Green (BioRad) Master Mix, 1 μ L of diluted forward and reverse primers (25 μ M in ddH₂O), and 3 μ L of ddH₂O. Samples were ran in the CFX-96 Connect Real-Time PCR Detection System (BioRad, Hercules CA) using cycling condition set at: 95°C for 2 min, 49 cycles of 95°C for 10 s, and 60°C for 20 s. Relative gene expression levels were calculated using the $2^{-\Delta\Delta C_t}$ method [105], with the Ct values normalized to *GAPDH*, and relative to healthy (vehicle).

Table 3: List of human primer sequences used in qPCR experiments

Gene	Forward Sequence 5' → 3'	Reverse Sequence 5' → 3'	Product size
<i>GPAT1</i>	TCG GGC AGG ACT TTT GTC AG	GGT TTG CCC AGT TGT TCA CC	135 bp
<i>GPAT2</i>	CAT CAG AAG CTC CTG GGG GA	GCC CAG AGA AGC CTA CAT CA	79 bp
<i>GPAT3</i>	GCC TCT GAG GGT TAC CTT GG	GAT CCG GCA GCA AGT CAG AT	133 bp
<i>GPAT4</i>	TGC CGG AAA GGA ATG GAG AC	CCA GTG CTA TCC TGA GCG G	193 bp
<i>AGPAT1</i>	AAC GTG GCG CCT TCC A	GAA GTC TTG GTA GGA GGA CAT GAC T	77 bp
<i>AGPAT2</i>	GGT ACT CGC AAC GAC AAT GG	TTG GTG TTG TAG AAG GAG GAG AAG	125 bp
<i>AGPAT3</i>	CTC TGG AGC CAA CTG GTC AT	GAG GAT GAT GAC TGC GTG CT	114 bp
<i>AGPAT4</i>	GCA CGG AAT GCA CCA TCT TC	CTT GGA GCC CCC TAA CAG C	149 bp
<i>CDS1</i>	GTG TTT GGA TTC AAT GCT GCC T	AGG GCT CAC ATT CTG TCA CG	106 bp
<i>CDS2</i>	CAG TCA GTC ATT GGC TGG AAA A	ATC CTC CAA AGG GGC CAA TG	100 bp
<i>PGPS</i>	GTC AAG CTC CAG AGG CTG TT	CAG CCA TGG TGA CCT AAG GA	95 bp
<i>CLS</i>	CTT GGT GGC AGC TTC TTT GG	GGC CCT GTT CCC ATT GAT GT	210 bp
<i>ALCAT1</i>	CAT GGT GTC ATG GAA AGG GA	TCC AAT AAT GCC ACA GGT AGG G	136 bp
<i>PPARα</i>	GCG AAC GAT TCG ACT CAA GC	AAA ACG AAT CGC GTT GTG TG	139 bp

Lipid extraction, Thin layer Chromatography (TLC), and Gas Chromatography (GC):

Healthy and Barth lymphoblasts treated with either 1 μ M of OEA or vehicle (0.1% ethanol) were grown in 75 cm² flasks at an initial seeding density of 10.8 million cells. Following the four-day growth period, cells from each flask was harvested into 50 mL Falcon tubes and centrifuged at 2000 \times g for 5 min. The supernatant was discarded, and the remaining cell pellet was washed two times with 2 mL of 1 \times PBS, in two centrifugation (2000 \times g for 5 min) and resuspension steps. Next, the supernatant was discarded one last time and the sample pellet was ready for lipid extraction.

Total lipids were extracted from lymphoblast samples using the Folch method as previously described [106, 107], with minor modifications. Briefly, lymphoblast pellets were suspended in 3 mL of 2:1 (v/v) chloroform/methanol, and vortexed at maximum speed for 1 min. This was followed by the addition of 500 μ L of Na_2PO_4 and subsequent inversion (x3). Thereafter, a centrifugation at $3000 \times \text{rpm}$ for 5 min separated the samples into two layers containing an organic and aqueous phase. The organic phase was removed and added to a fresh tube, and the aqueous phase underwent two additional Folch extractions to ensure minimal loss of total lipids from each sample. Once the additional two aqueous phases are added to the previous fresh tube, it was dried under an N_2 stream, and resuspended in 50 μ L of chloroform.

To isolate individual phospholipid species, the samples were reconstituted in chloroform and applied onto a thin-layer chromatography plate (Silica Gel Hf, 20 x 20 cm, 250 μ M; Analtech Inc.) using a Hamilton syringe and resolved on a chloroform:methanol:2-propanol:0.25% KCl:trimethylamine solvent system (30:9:25:6:18, v/v/v/v/v) [106]. Individual phospholipid bands were visualized under a UV light source after spraying with 0.1% 2,7-dichlorofluorescein in methanol (w/v) and compared with external bovine cardiolipin standard (Avanti Polar lipids). The corresponding cardiolipin bands were overlaid with docosatrienoic acid (22:3n-3) ethyl ester, as an internal standard (Nu-Check Prep, Elysian MN), then scraped and extracted for the determination of cardiolipin composition by gas chromatography [108].

In preparation for gas chromatography, the fatty acyl species within the scraped cardiolipin bands were derivatized to fatty acyl methyl esters by a transesterification method using 14% boron trifluoride in methanol and hexane (Thermo Scientific, Bellfonte PA). This was then heated on a heat block at 95°C for 1 h [108]. Following centrifugation at $3000 \times \text{rpm}$ for 5 min, the top layer was moved into a fresh tube, dried under a N_2 stream, and resuspended in 65

μL of heptane. Subsequent analysis using gas chromatography with flame ionization detection have been conducted by Mr. Daniel Chalil at the Laboratory of Nutritional Lipidomics using the Varian 3900 gas chromatograph equipped with a DB-FFAP 15 m x 0.10 mm injected dose x 0.10 μM film thickness nitroterephthalic acid-modified polyethylene glycol capillary column (J&W Scientific/Agilent Technologies, Mississauga, Ontario, Canada). To complete this work, Mr. Chalil used the fast gas chromatography protocol as described previously [109]. Here, the fatty acyl composition was expressed as both concentrations (μg fatty acids per 10⁷ cells) and relative weight percentages (as a percentage of total fatty acid mass analyzed), and the total cardiolipin content was calculated based on the total mass of all cardiolipin fatty acyl species within each sample.

Statistical Analysis:

Data are expressed as means ± S.E.M, or as individual values. Repeated measures two-way analysis of variance (ANOVA) with multiple comparisons using Sidak's post-hoc test was used to analyze for the effects of treatments within cell types, and effects of cell type within each treatment. In addition, interactions between cell types and treatments were assessed using a two-way analysis of variance (ANOVA) with Tukey's multiple comparisons post-hoc test. Differences between treated and untreated cells for individuals were assessed by Student's paired t-test. Significant differences were accepted at P<0.05.

Results:

BTHS lymphoblasts have higher mRNA expression of *PGPS*, *CDS1*, and *GPAT3* as compared to healthy lymphoblasts. OEA partially normalized this effect. Quantitative PCR was used to investigate the underlying differences in mRNA expression levels of genes involved in cardiolipin biosynthesis between BTHS and healthy lymphoblasts, and to also determine if OEA has any effects to alter these genes. BTHS or healthy cells (1.2 million per flask) were treated with vehicle or OEA, grown for 96 hours, before being harvested and analyzed by RT-qPCR for relative mRNA expression of genes involved in cardiolipin biosynthesis. All gene expression values were normalized to *GAPDH*.

Comparing between vehicle treated healthy lymphoblast and vehicle treated BTHS lymphoblast (Fig. 6), a majority of the tested CL synthesis genes were not differently expressed. Only one significant difference was evident. *CDS1* mRNA levels were ~9 folds higher in BTHS lymphoblasts compared to healthy control lymphoblasts. *GPAT3* and *PGPS* mRNA expression levels were also higher in BTHS lymphoblast relative to healthy lymphoblast by about 7 folds and 2.2 folds, respectively, but this was not statistically significant. No significant differences in mRNA expression of CL synthesis gene were observed between vehicle treated and OEA treated healthy lymphoblasts. Treatment with OEA significantly decreased *CDS1* mRNA expression in BTHS lymphoblasts, so that it was no longer significantly different compared to vehicle treated healthy control. OEA also had a partial effect to decrease *GPAT3* and *PGPS* mRNA expression in BTHS lymphoblast by nearly 2.2 and 0.6 folds, but this was not statistically significant. No additional effects were observed.

OEA treatment did not increase total cellular CL content in BTHS lymphoblast.

One set of BTHS and healthy lymphoblasts (GM22192 & AG15022) were treated with vehicle

or OEA for a total of 96 hours and then harvest and extracted for total lipids. Individual phospholipids were resolved by TLC, and the bands corresponding to known cardiolipin standard were scraped and analyzed by GC, to determine the total CL mass per 10 million cells for each treatment group. As expected, vehicle treated healthy lymphoblasts had a higher total CL content compared to BTHS treated lymphoblast, by 18% (vehicle healthy, 4.55 μg of FA of CL/ 10^7 versus vehicle BTHS, 3.76 μg of FA of CL/ 10^7). Surprisingly, the treatment with OEA did not increase the CL content of BTHS lymphoblast, and instead caused a slight decrease in CL by $\sim 9\%$ (OEA BTHS, 3.41 μg of FA of CL/ 10^7 versus vehicle BTHS, 3.76 μg of FA of CL/ 10^7).

OEA treatment of BTHS lymphoblast did not alter the relative content of individual fatty acids in CL. The relative proportions of individual fatty acids within the CL of one set of BTHS and healthy lymphoblasts treated with or without OEA was quantified and determined by GC-FID. Analysis of major fatty acyl classes in CL revealed higher relative SFA content, lower MUFA content, lower n-6 PUFA content, and higher n-3 PUFA content, in both vehicle- and OEA-treated BTHS lymphoblasts as compared to vehicle- and OEA-treated healthy lymphoblasts. No major differences were observed when vehicle-treated healthy and OEA-treated healthy or vehicle treated BTHS and OEA treated BTHS was compared.

The relative levels of individual fatty acyl species within CL between each group were examined and several differences were apparent. More specifically, lower relative contents of oleic acid (C 18:1n-9), palmitoleic acid (C 16:1), linoleic acid (C 18:2n-6), and dihomo-gamma-linolenic (C 20:3n-6) were apparent in both vehicle- and OEA-treated BTHS lymphoblast as compared to vehicle- and OEA-treated healthy control, which got shifted to relative higher levels of vaccenic acid (18:1n-7), palmitic acid (16:0), and steric acid (18:0). OEA had very minor

effects and did not alter the relative contents in any of the above aforementioned fatty acids, in both healthy and BTHS lymphoblast. Additional information on the absolute mass of individual fatty acyl species within the CL of BTHS and healthy lymphoblast are illustrated in **Appendix Fig. 3**.

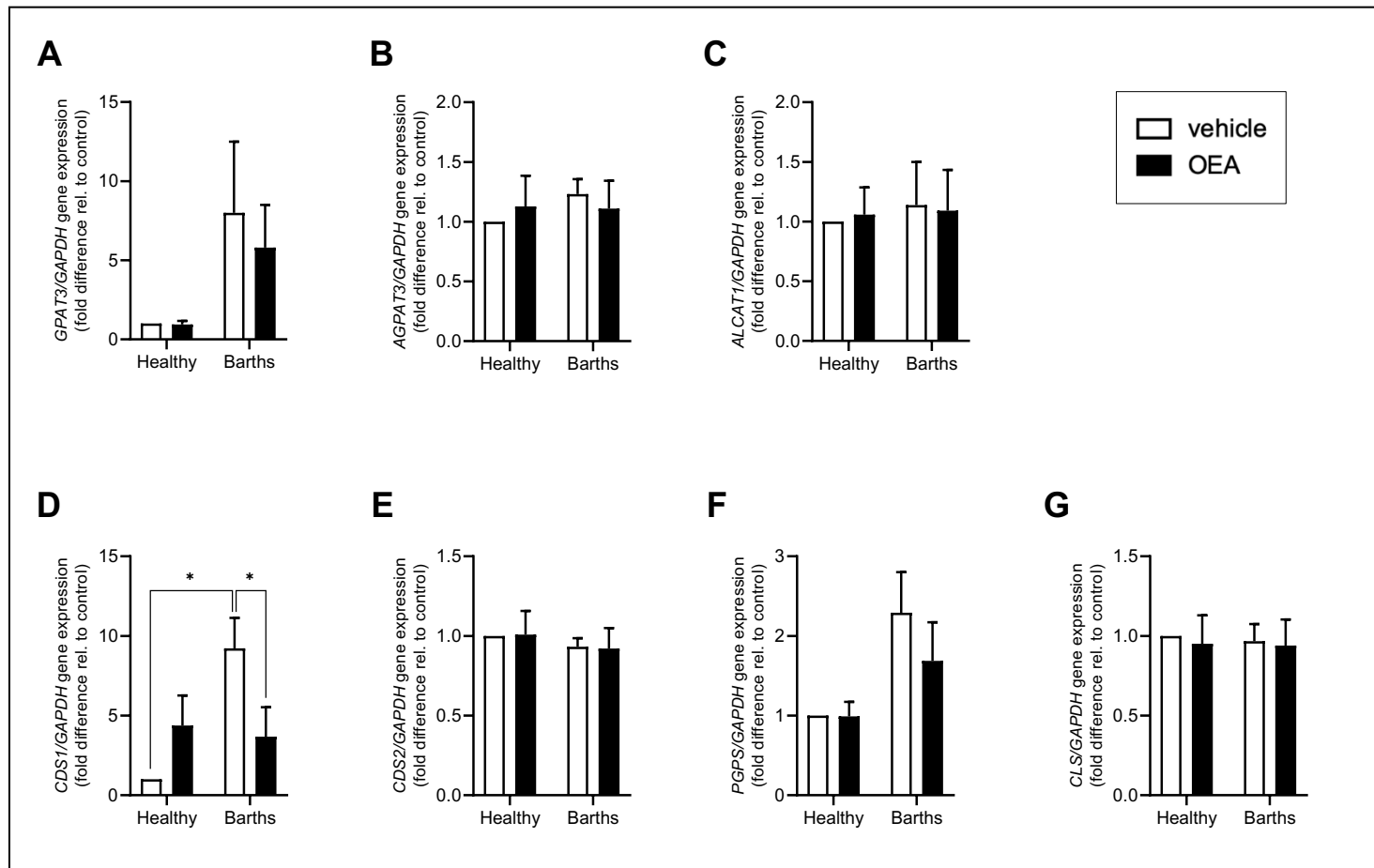


Figure 6: Expression of related cardiolipin biosynthetic/remodelling genes in vehicle and OEA treated healthy and Barth's lymphoblasts.

(A) *GPAT3* - Glycerophosphate acyltransferase 3, (B) *AGPAT3* – Acylglycerolphosphate acyltransferase 3, (C) *ALCAT1* - Acyl-CoA: lysocardiolipin acyltransferase 1, (D) *CDS1* - Phosphatidate cytidyltransferase 1, (E) *CDS2* - Phosphatidate cytidyltransferase 2, (F) *PGPS* - Phosphatidylglycerol phosphate synthase, (G) *CLS* – Cardiolipin synthase. Analysis was performed using repeated measures two-way ANOVA to analyze for effects of treatment within cell types, and the effects of cell types within treatments, with Sidak's multiple comparisons test. Two-way ANOVA with Tukey's multiple comparisons test was further used to analyze for interactions between cell types and treatments. Data are mean \pm S.E.M., *P<0.05, n=3, biological replicates.

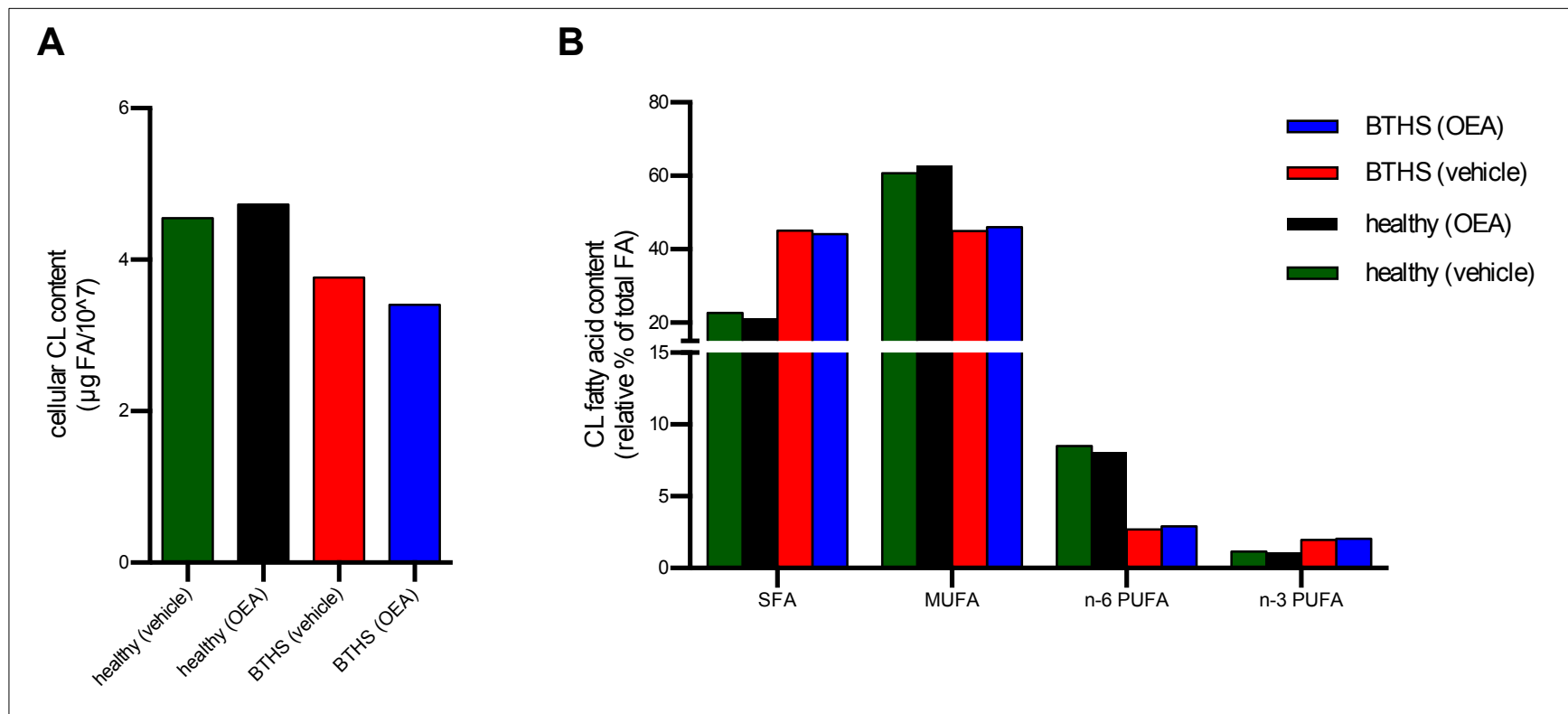


Figure 7: Preliminary cardiolipin analysis of a single set of BTBS and healthy lymphoblasts (GM22163 & AG14750), treated with OEA or vehicle.

(A) Endogenous CL content of lymphoblast derived from BTBS patients or healthy controls treated with vehicle or OEA for 96 hours (n=1). **(B)** Relative % of major fatty acid classes (i.e. SFA, MUFA, PUFA) within CL from healthy and BTBS lymphoblast treated with either OEA or vehicle (n=1, biological replicates).

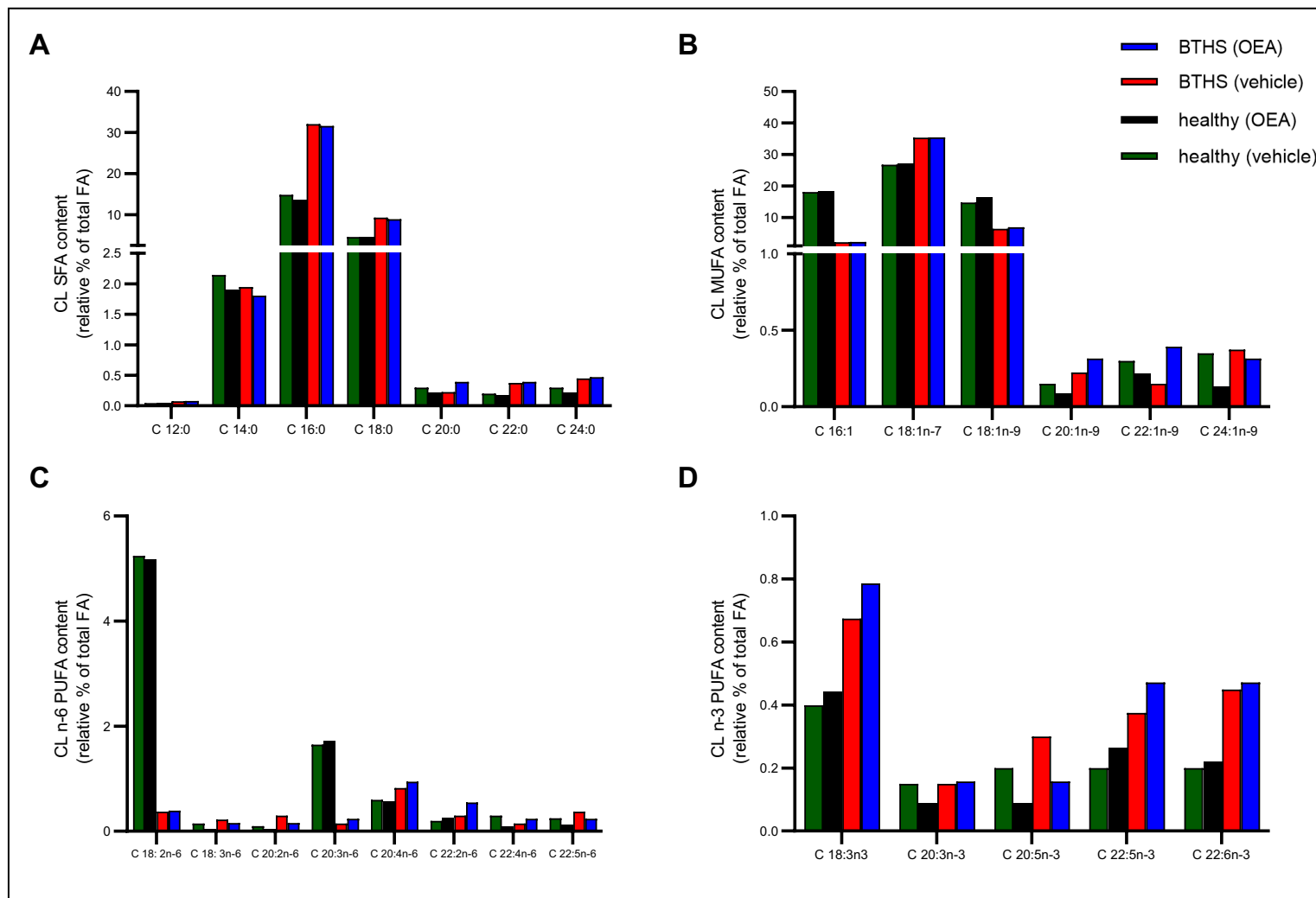


Figure 8: Fatty acyl profile of CL isolated from a single set of BTHS and healthy lymphoblasts (GM22163 & AG14750) treated with or without OEA.

Relative proportions of individual fatty acyl species within CL from cultured healthy and BTH lymphoblasts treatment with vehicle or OEA for 96 hours. **(A)** SFA species, **(B)** MUFA species, **(C)** n-6 PUFA species, **(D)** n-3 PUFA species, n=1, biological replicates.

Discussion:

The primary aim of this thesis chapter was to determine if the effects of OEA on BTHS lymphoblast cell number was associated with changes in CL metabolism. To help clarify this mechanism, two separate studies were conducted that focused on the differences in mRNA expression of genes involved in cardiolipin biosynthesis, and the differences in cardiolipin content and fatty acyl composition, between BTHS and healthy lymphoblasts treated with or without OEA.

In the first set of experiments, the mRNA expression level of *CDS1* was shown to be higher in vehicle-treated BTHS lymphoblasts compared to vehicle-treated healthy controls. This likely indicates a compensatory response by BTHS cells to drive up the *de novo* synthesis of CL, in order to restore the observed deficit in cellular CL levels. However, despite the upregulation of these genes, CL content was still reported to be lower in BTHS lymphoblasts when compared to healthy control [96]. This suggests that any potential increase in CL synthesis was unable to keep up with the impaired regeneration of CL from MLCL or DLCL.

Subsequently, the effect of OEA on the expression levels of genes involved in CL biosynthesis in both BTHS and healthy lymphoblasts were also compared. The treatment with OEA had a normalizing effect to decrease the expression levels of *CDS1*, so that they were not different from healthy OEA-treated control and healthy vehicle-treated control levels. In theory, a decrease in mRNA expression of genes involved in CL synthesis should normally cause a direct decrease in CL production, which would be detrimental to cells with CL deficiency. However, it could also be speculated that the treatment of OEA might have restored the CL content in BTHS cells, perhaps through the increased remodeling of MLCL back to mature CL. Thus, the upregulation of genes was no longer necessary. Given these assumptions, additional

experiments were then planned to confirm if OEA can increase cellular CL content in BTHS lymphoblast, and if this increase is associated with alterations in CL fatty acyl composition.

To examine the effects of OEA on CL content, one set of BTHS and healthy lymphoblast lines treated with OEA or vehicle were analyzed. As expected, vehicle treated BTHS lymphoblast had 18% less CL mass when compared with vehicle treated healthy control, which agreed with previous observations in literature [96]. Interestingly, the treatment with OEA did not increase the total CL content of BTHS lymphoblast, but instead had an opposing effect to further decrease CL content by about 9%. Seeing that the endogenous CL biosynthesis significantly increased following PPAR α activation in cardiac cells [89], it is surprising that OEA, a potent activator of PPAR α , was unable to elicit positive effects on Barth lymphoblast CL. This may be attributed to the fact that lymphoblasts and cardiac cells are very different cell types, with different functions and metabolic activity. Thus, their responsiveness to PPAR α activation might be innately different. However, given that only a single analysis was conducted, it is difficult to draw conclusions without reproducing the data. Notably, this finding was different the result found previously, which did show a small positive effect of OEA on total CL content in BTHS lymphoblasts, and which was reported in the PhD thesis of Dr. Ryan Bradley [85]. The reason for this discrepancy is unknown. Regardless, it will be important to reproduce these data, and add additional samples, before any conclusions can be drawn.

Next, the relative proportions of individual fatty acids within CL were quantified in both healthy and BTHS lymphoblasts treated with OEA or vehicle, to determine if OEA can alter the CL fatty acyl composition of BTHS lymphoblasts. Similar to the previous characterization data by Michael Schlame's research group [52], the most abundant fatty acyl species within the CL of healthy lymphoblasts were vaccenic acid, palmitoleic acid, oleic acid, and palmitic acid. BTHS

caused a major shift in the relative abundance of individual fatty acid within CL, such that palmitoleic acid and oleic acid levels were replaced by higher levels of vaccenic acid, palmitic acid, and steric acid. The treatment with OEA once again had minimal effects, as it did not change the relative levels of any of the major fatty acyl species with BTHS lymphoblast. Considering that only one set of BTHS and healthy lymphoblast sample was analyzed to date, more biological replicates are clearly needed to confirm the effect of OEA on the CL content and composition of additional BTHS lymphoblast donors. Nonetheless, preliminary results from this study suggested that the effects of OEA on lymphoblast cell number was not likely mediated by changes in CL content or composition. Thus, further experimentation is needed to determine if the effects of treatment with OEA was mediated by other factors.

Chapter Five: Thesis Study III – Effect of OEA on BTHS Lymphoblast Mitochondrial Number, Size, and Morphology

Study Rationale

Although based on an n=1, findings from study II demonstrated that the treatment with OEA did not substantially increase the total CL content of Barth lymphoblast, or alter its CL fatty acyl profile, suggesting that the positive effects of OEA on increased BTHS lymphoblast number was instead mediated by another factor. OEA is an agonist of TRPV1 and PPAR α . Given that both have been previously been shown in literature to play a regulatory role in mitochondrial processes such as mitochondrial biogenesis and fission [110, 111], it is possible that the effect of OEA on BTHS lymphoblasts could instead be mediated by the direct modulation of the mitochondria.

Previous characterization of the mitochondrial ultrastructure of BTHS lymphoblasts, reported reduced parallel cristae structure, decreased cristae density, and increased numbers of giant swollen mitochondria often with “honeycomb like” or “onion-shaped” structures [68, 96]. These changes were reported in conjunction with an overall reduction in mitochondrial membrane potential and electron transport activity [52, 96]. Consequently, there was also evidence of the hyperproliferation of BTHS mitochondria, possibly to compensate for the decreased energy production [68]. Since proper mitochondrial health is critical to cell survival, and the mitochondrion is the central regulator of cell death [94, 112], it is thus, of interest to examine if OEA has any effects to repair the observed mitochondrial abnormalities in BTHS lymphoblasts, so that it is more comparable alongside healthy controls. This avenue of investigation may provide new insight into help explain the mechanism behind the positive effects of OEA treatment on BTHS lymphoblast number. Thus, the overarching objective of this

thesis chapter was to determine treatment effects of OEA on BTHS mitochondrial size, shape, and cristae morphology, and whether OEA treatment can increase similarity to healthy controls.

Objectives and Hypothesis

Objective: To determine if the treatment with OEA will restore the abnormalities observed in mitochondrial number, size, shape, and total cristae length of BTHS lymphoblast, so that they are more comparable to healthy controls.

Hypothesis: BTHS lymphoblasts will have greater mitochondrial number and size, less average cristae length, more circular shape, and greater ratio of giant mitochondrial, as compared to vehicle healthy controls. OEA treatment will partially normalize all of the aforementioned differences to healthy control levels. There will be no major differences between treated and untreated healthy lymphoblasts.

Methods:

Transmission Electron Microscopy

The following protocol is adapted from Acehan et al. (2007) [68]. To begin, healthy and Barth lymphoblasts were treated with 1 μ M of OEA or vehicle (0.1% ethanol) and grown in a 25cm² flasks at an initial seeding density of 1.2 million cells. Following a four-day growth period (96 hour), the cells were harvested into 50 mL Falcon tubes and centrifugated at 1000 \times g for 5 min. The supernatant was removed, and the cells were washed three times with 1 mL of 1 \times PBS via a series of centrifugation (1000 \times g for 5 min) and resuspension steps. Following the final wash, the supernatant was discarded, and the sample pellet was fixed in 1 mL of a 2.5% glutaraldehyde solution (mixed in 1 \times PBS), and then stained for 1h in a 0.5% Osmium Tetroxide solution (mixed in 1 \times PBS). After undergoing a series of graded dehydration steps using acetone: 20% (10 min), 50% (10 min), 70% (10 min \times 2), 90% (10 min \times 2), and 100% (10min \times 2), each sample was embedded onto an Epon-Araldite (E/A) resin (DDSA liquid 30.0 g, Araldite 502 11.1 g, TAAB embedding resin 15.5 g, DMP 30 1.4 g). Our collaborator Mishi Groh, who is the TEM technician for the University of Waterloo Biology Department, sliced ultrathin sections (~10nm) from the resin and collect it onto a carbon-coated grid. Finally, I collaborated with Ms. Groh at the University of Waterloo Electron and Confocal Microscopy Facility and collected high resolution images of the lymphoblast samples.

As for the sampling approach, approximately 20 ultrathin sections were obtained for each treatment group. Out of these sections, one was chosen at random and imaged with the Phillips CM10 Transmission Electron Microscope, to get a detailed cross-sectional view of the cells. Cells were then selected and imaged at random areas of the electron micrograph and saved for further analysis. In the first BTHS and healthy lymphoblast set, roughly 7 cells were imaged for

the healthy-vehicle group, the BTHS-vehicle group, and the BTHS-OEA group and 3 cells were imaged for the healthy-OEA group. In the second set, two cells were imaged for each four treatment groups.

Further analysis was performed using the ImageJ software (version 1.8.0_112), with added macros provided by Springer Protocols (2019). Very briefly, each cell image was analyzed for mitochondrial number, size, shape, and cristae length. Mitochondrial number per cell was normalized to the size of the nucleus to account for differences in sectioning area between cells. Size was determined based on the average of all areas taken up by mitochondria in μm^2 . Shape was analyzed using the added macro circularity tool, where a value of one indicates a perfect circle, and a value approaching 0 indicates an increasingly elongated shape. Average cristae length was calculated based on the sum of the total cristae length in micrometer divided by the total number of mitochondria. Importantly, the cristae need to be parallel in nature, and must be connected to the inner boundary membrane in order to be included into the analysis. Mitochondrial density was measured based on the multiplication of mitochondrial number and size, normalized to the size of the nucleus. Finally, each outcome measure was then averaged over the total number of cells within each treatment group in both set of BTHS and healthy donors.

Results:

BTHS lymphoblasts have less cristae length and greater mitochondrial size as compared to healthy lymphoblasts. Underlying differences in mitochondrial ultrastructure were compared between two sets of BTHS and healthy lymphoblast lines (GM22192, GM22163, AG15022, & AG14750). Following 96 hours of growth, each treatment group was harvested and prepared for transmission electron microscopy imaging, and additional analysis was performed using ImageJ. For BTHS donors sets (GM22192 & GM22163), both were shown to have lower average cristae length and higher average mitochondrial size per cell, when compared to healthy donors (AG15022 & AG14750) (**Fig. 10**). Differences can be observed in mitochondrial size measurements, such that BTHS donor (GM22163) was shown to have higher average number of mitochondria per cell compared to both healthy donors (AG15022 & AG14750), whereas, BTHS donor (GM22192) was shown to have similar mitochondrial number compared to healthy donor (AG15022), and less mitochondrial number compared to healthy donor (AG14750) (**Fig. 10**). Furthermore, the ratio of mitochondria that is greater than $1\mu\text{m}^2$ was also greater in the two BTHS lymphoblast lines compared to healthy lymphoblast lines (GM22192 (20%) & GM22163 (12%) versus AG15022 (5%) & AG14750 (0%)) (**Fig. 10**), and finally, no major differences was observed in circularity (**Fig. 10**).

OEA treatment of BTHS lymphoblast increased mitochondrial number and decreased mitochondrial size. When examining the effects of OEA on the mitochondrial ultrastructure of BTHS lymphoblasts, several differences were apparent. First of all, OEA treatment increased the average mitochondrial number per cell of BTHS lymphoblasts from two distinct donors (GM22192 & GM22163), and had an opposing effect to decrease the average mitochondrial size, so that these measures became more comparable to healthy control levels

(Fig. 10). While OEA did increase the average cristae length of both BTHS lymphoblast donors, it only partially corrected this, as the deficit in total cristae length between OEA treated BTHS lymphoblast and vehicle control lymphoblast were as high as 75.3% for GM22192 and 43.8% for GM22163 **(Fig. 10)**. Perhaps the largest effect of OEA treatment comes from the ratio of mitochondria that is over $1\mu\text{m}^2$. OEA decreased the percent of total mitochondrial larger than $1\mu\text{m}^2$, from 20% to 5% in the BTHS donor (GM22192), and 12% to 0% in the BTHS donor (GM22163) **(Fig. 10)**. No major effects were observed in circularity and mitochondrial density between OEA and vehicle treated BTHS lymphoblast **(Fig. 10)**.

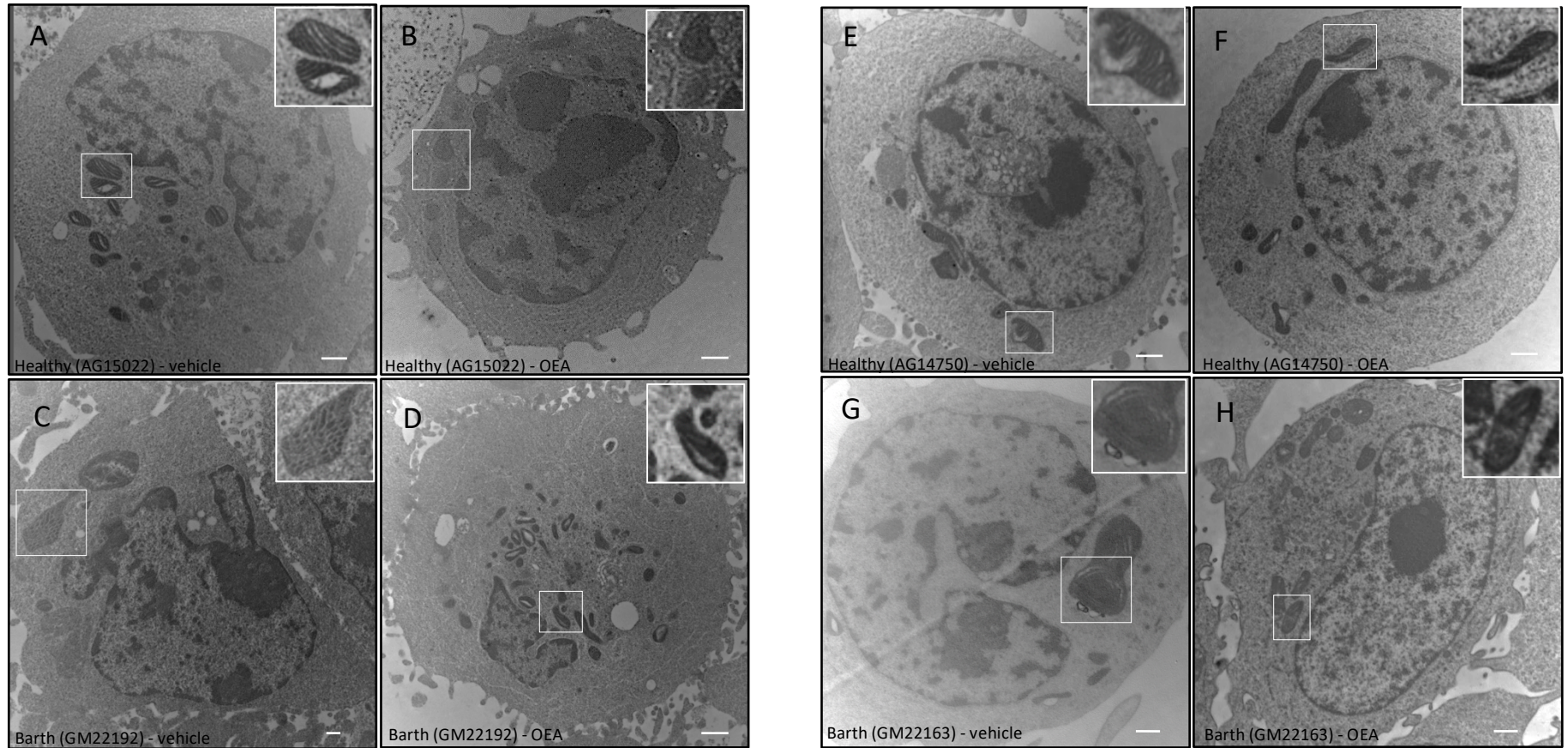


Figure 9: Transmission electron microscopy images of lymphoblasts derived from BTHS (GM22192 & GM22163) and healthy (AG15022 & AG14750) donors.

Cross-sectional view of one representative cell from each BTHS and healthy lymphoblasts treated with vehicle or OEA, respectively. (A,B) Healthy-AG15022, (C,D) BTHS - GM22192, (E,F) healthy - AG14750, (G,H) BTHS - GM22163, scale bar = 0.5 microns.

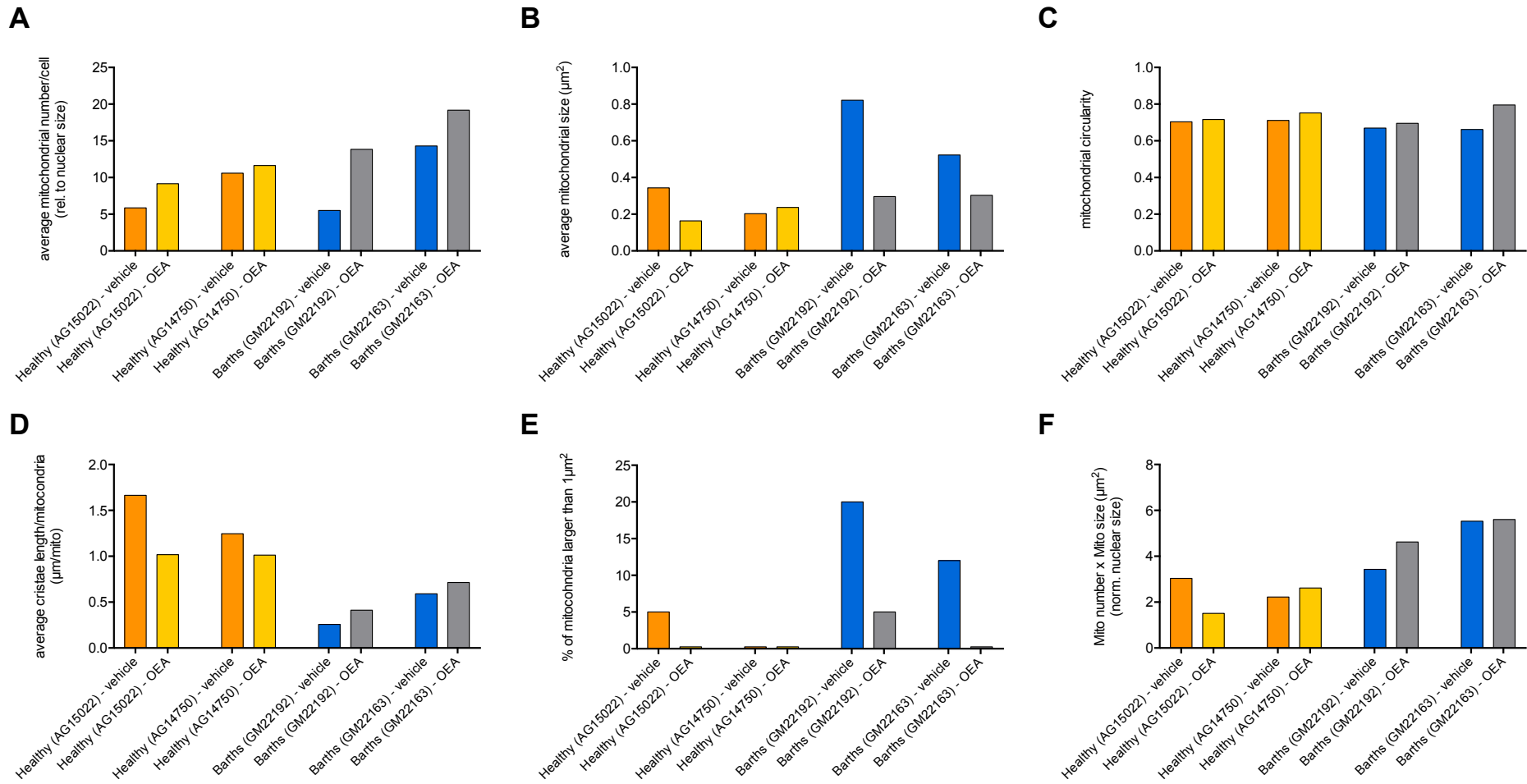


Figure 10: Additional analysis of the transmission electron microscopy images of lymphoblasts derived from two sets of BTHS (GM22192 & GM22163) and healthy (AG15022 & AG14750) donors, treated with vehicle or OEA. (A) average mitochondrial number, (B) size, (C) shape, (D) average cristae length, (E) % of mitochondria larger than $1\mu\text{m}^2$, and (F) mitochondrial density from two set of BTHS and healthy lymphoblasts donors treated with OEA or vehicle, $n=1$, average values are shown for one individual (*i.e.* one biological replicate).

Discussion:

The primary objective of this thesis chapter was to determine if the treatment with OEA will have any major effects on mitochondrial number, size, or morphology of BTHS lymphoblasts. To help answer this question, transmission electron microscopy was used to take detailed images of two distinct sets of BTHS and healthy lymphoblasts lines, treated with either OEA or vehicle, to analyze for differences in mitochondrial number, size, shape, and cristae length.

As expected, BTHS lymphoblast had drastically lower cristae length in comparison to healthy lymphoblast controls. This difference was probably attributed to the observed deficiency in CL content of BTHS, which causes cristae misalignment and destabilization [68]. As for mitochondrial size, BTHS lymphoblast are much larger than healthy controls, with a higher percentage of giant mitochondria over the size of $1\mu\text{m}^2$. This result was congruent with past BTHS imaging studies, which described the increased accumulation of giant mitochondria with abnormal “honey-comb” or “onion-shaped” morphology [68].

Since the reason behind the enlargement of BTHS mitochondria has yet to be determined, I proposed in this study that the increase in size could be due to an imbalance between mitochondrial dynamics. Seeing that the activation and function of DRP1 requires the direct binding of CL [41], the observed BTHS deficiency in CL may lead to a decreased ability of the DRP1 protein to facilitate fission. On the other hand, CL is involved in mitochondrial fusion, through the direct binding to OPA1 protein [42]. However, the ability of OPA1 to oligomerize into its active state has been shown to remain unchanged between BTHS and healthy lymphoblasts [96]. This suggest that OPA1 may be able to function despite CL deficiency. Therefore, the increase in mitochondrial size as observed in BTHS lymphoblasts was possibly

due to the combined effects of decreased fission, in-conjunction with a normal ability to initiate fusion. As for mitochondrial number, an expansion of the mitochondrial volume was previously described, which was indicative of mitochondrial hyperproliferation [52]. However, results from my study only partially agreed with this notion, as only one BTHS lymphoblast donor had a higher average mitochondrial count relative to healthy donor (GM22163 and AG14750). Finally, no major differences were observed in overall mitochondrial circularity between BTHS and healthy lymphoblasts, suggesting that CL deficiency does not lead to any abnormal changes in mitochondrial shape.

The next major focus of this study, which was to determine the effects of OEA on mitochondrial number, size, shape, and cristae length of BTHS lymphoblast. In this regard, the treatment with OEA only had a minor effect to increase the length of parallel cristae in BTHS, which was still not near the levels observed in healthy controls. This result was not surprising, because I did not find a major effect of OEA on either CL content or composition. Therefore, it seemed unlikely that OEA would have any major effect on BTHS cristae morphology. On the contrary, the treatment with OEA was shown to have impacts on several other outcome parameters, such that OEA increased the average number of mitochondria per BTHS cell by nearly 151% in BTHS donor (GM22192), and 34% in BTHS donor (GM22163). Furthermore, OEA also had a normalizing effect to decrease the average size of BTHS mitochondria by nearly 173% in GM22192, and 67% in GM22163, so that the difference between BTHS and healthy was no longer prominent. Possibly the largest effect was observed in the ratio of giant mitochondria, in which the treatment with OEA decreased the percentage of mitochondria that is larger than $1\mu\text{m}^2$ from 20% to 5% in the BTHS donor set (GM22192), and from 12% to 0% in the BTHS donor set (GM22163).

While the previous section did highlight the two major effects of OEA to alter the number and size of mitochondria from BTHS lymphoblasts, the direct mechanism behind how these changes lead to the observed increase in BTHS cell growth still needs to be clarified. According to the literature, two of the receptor agonists of OEA (PPAR α and TRPV1) have both been shown to be involved in the induction of mitochondrial fission [110, 113]. More so, the direct treatment of Bezafibrate, a PPAR α agonist, increased the rate of fission in mitochondria of DRP1-deficient skin fibroblasts, which lead to an overall increase in fibroblast growth [113]. Given this result, it is suggested that the effects of OEA to decrease BTHS mitochondrial size, was probably due to the enhanced fission as well. Since mitochondrial fission events are known to be a vital process during the M phase of the cell cycle to ensure equal distribution of mitochondria to both daughter cells [114], a DRP1 inhibition has been shown to cause a significant reduction in the proliferative abilities of T cells, thymocytes, fibroblasts and many cancer cells [113, 115-118]. Based on these findings, BTHS cells with decreased fission capacity will be expected to have difficulty progressing through the cell cycle to undergo cell division. Thus, the potential underlying effects of OEA to promote mitochondrial fission, might be an important contributing factor to an increase in BTHS lymphoblast proliferation (**fig. 11**). In an alternative pathway, the effects of OEA on lymphoblast number could also be mediated by an increase in mitophagy, since the induction of fission has been shown previously to be an essential initiating step prior to autophagosome formation [119]. More so, the inhibition of Drp1 directly lead to a 75% decrease in the number of autophagosomes containing mitochondria [120]. Therefore, the ability of OEA to promote mitochondrial fission, may allow for an increased turnover of depolarized mitochondria with ROS accumulation, to prevent BTHS lymphoblast cell death (**Fig. 11**).

Data from study III may also help to explain how the increase in mitochondrial number lead to an overall increase in BTHS lymphoblast growth. Prior works using a TRPV1 agonist (Capsaicin), increased the expression of PGC-1 α , which was accompanied by an increase in mitochondrial biogenesis and respiration [121]. Similar effects were also observed in a BTHS animal model using TAZ-deficient mice, where the treatment with a PPAR α agonist (Bezafibrate) promoted mitochondrial biogenesis of cardiomyocytes and increased the enzymatic activity of complex I-III, through the co-activation of PPAR α and PGC-1 α [111]. Based on these findings, it is suggested that the effects of OEA on BTH mitochondrial number may be mediated by an increased activation of PGC-1 α to promote mitochondrial biogenesis. Since the overexpression of PGC-1 α has been previously implicated to be protective against oxidative stress related cell death, through the combined effects of improved mitochondrial membrane potential and decreased ROS [122-124], it is possible that the induction of OEA on PGC-1 α may lead to decreased lymphoblast cell death. Surely, an increase in mitochondrial number could also improve the overall efficiency of cellular respiration, to provide ATP for the energy demanding process of cell division [102]. Therefore, another proposed mechanism for the effects of OEA to increase BTHS cell number, is likely mediated by an increased expression of PGC-1 α to promote mitochondrial biogenesis, which will either improve cell proliferation or decrease ROS mediated cell death (**Fig. 11**).

To summarize, BTHS lymphoblasts were shown to have initial evidence of decreased cristae length, increase mitochondrial size, and a greater ratio of enlarged/giant mitochondria. I theorize that the mechanism behind the effects of OEA to increase the number of BTHS lymphoblast cells was likely mediated by an increase in mitochondrial fission, and an increase in

PGC-1 α induction, leading to either decreased BTHS lymphoblast cell death or increase BTHS lymphoblast proliferation. Future work should directly investigate this mechanism.

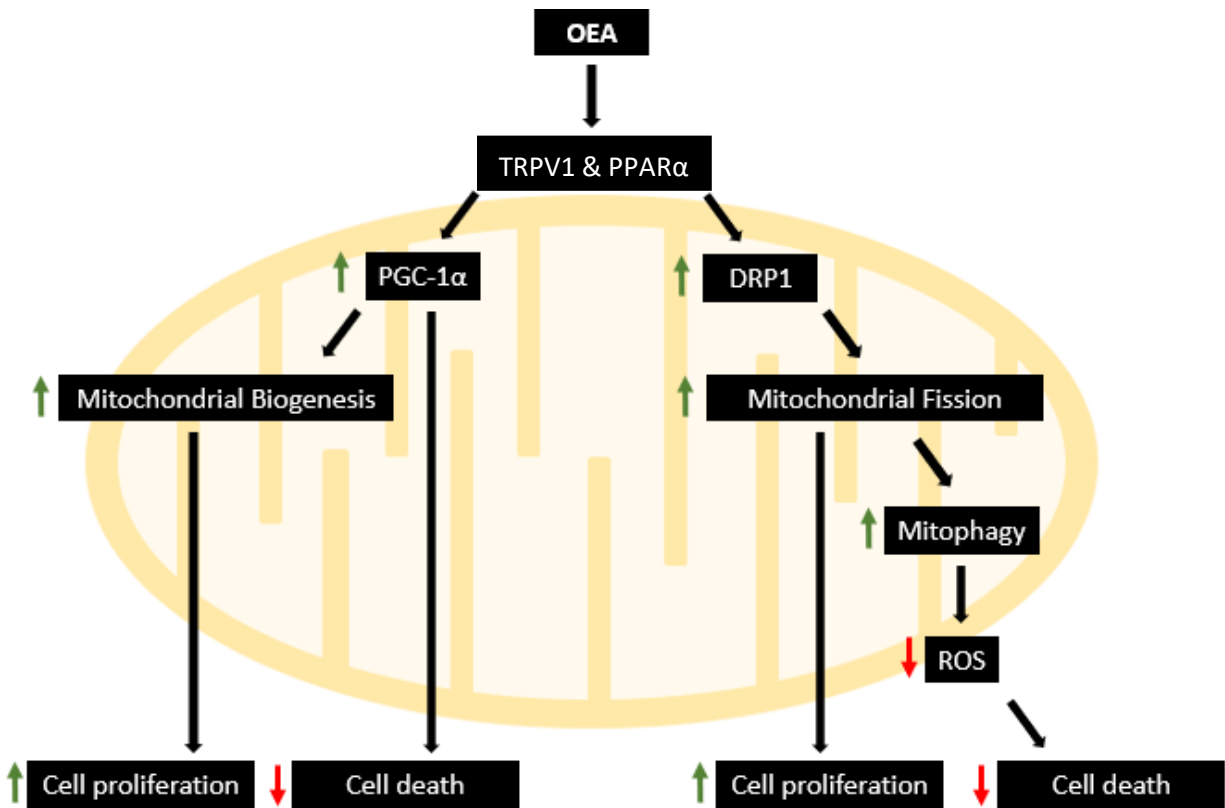


Figure 11: Proposed mechanisms for the effects of OEA to increase BTHS lymphoblast cell number.

The treatment with OEA targets PPAR α and TRPV1 to enhance the expression of PGC-1 α . PGC-1 α then induces mitochondrial biogenesis to promote cell proliferation. Alternatively, PGC-1 α overexpression may also lead to decreased ROS production and enhanced mitochondrial membrane potential to prevent cell death. In a separate pathway, PPAR α and TRPV1 induction leads to increased DRP1 activity to promote mitochondrial fission, which will lead to increase cell proliferation. Furthermore, increased mitochondrial fission may also lead to greater mitophagy for the clearance of mitochondria with ROS accumulation, to promote overall cell survival.

Chapter Six: Thesis Summary, Integration, and Conclusion

The overall aim of this thesis was to assess the capacity of OEA or LEA as potential therapeutic agents in treating one aspect of immunodeficiency in BTHS. For this purpose, three primary objectives were investigated, which focused on the effects of treatment on BTHS lymphoblast cell number, CL content and composition, and mitochondrial number, size, and morphology.

Until now, much of the clinical data on BTHS immunity has focused specifically on the innate immune system, with studies suggesting a decrease in neutrophil count that is likely due to increased myeloid progenitor cell apoptosis and/or myeloid cell maturation arrest, but that occurs cyclically [7, 9-12]. However, little is still known regarding the effects of BTHS on the adaptive immune system, and whether or not BTHS patients also manifest symptoms of lymphopenia. Clinical studies on the adaptive immune system present challenges. Among circulating leukocytes, the normal percentage of lymphocytes only account for, at most, ~30% of all leukocytes, although this can increase to as high as 40% during viral and bacterial infection [125, 126]. Thus, the optimal time to analyze BTHS lymphocyte function is when patients are undergoing an immune response from a recent infection. However, patient recruitment during this phase is both difficult and, given the impaired immunity in this cohort, unethical. Furthermore, due to the cyclical nature of immune cell crashes, the mechanistic study of lymphocyte precursors, such as lymphoblast and lymphoid progenitor cells, requires bone marrow aspiration [127]. This process can be invasive and dangerous for BTHS patients with clinical symptoms of neutropenia, which has further limited the active study of a possible lymphopenia in these patients. Taken together with the very small patient population available,

these factors have resulted in a deficiency of clinical data on the impacts of BTHS on lymphocyte and lymphocyte precursors in the literature.

Given this knowledge gap, I used lymphoblast cell lines derived from boys with BTHS and determined that there was a significant deficit in the ability of these cell lines to increase in number over time compared to healthy controls, which has not yet been reported, to the best of my knowledge. These data agree with the recent unpublished findings of other labs, which was communicated during the 2020 BSF Scientific and Medical Symposium. During that meeting, other groups reported observing lymphopenia in the Tafazzin deficient mouse model, as evidenced by reduced T and B lymphocyte counts [13]. However, those groups had not yet discovered the mechanism underlying the reduction in lymphoid-derived cells in *Taz* deficient mice, and our group has not yet determined the mechanism underlying the reduced rate of cell increase of cultured B-lymphoblasts derived from BTHS patients. Taken together, however, these data suggest deficits either in the proliferation or survival of progenitor cells. In addition, future experiments should focus on examining the capacity of BTHS lymphoblasts to differentiate into mature lymphocytes, to determine if lymphoblasts have maturation arrest alongside deficiencies that limit cell number.

The primary focus of this thesis was investigation of the efficacy of OEA and LEA in resolving the impairment in BTHS B-lymphoblast cell number expansion, which would suggest a potential therapeutic role for these compounds in treating the lymphopenia observed *in vivo* with *Taz* deficiency. I observed that the treatment with OEA by day three and day four partially restored the deficit in cell number of five distinct BTHS lymphoblast donors, whereas the treatment with LEA did not significantly restore the number of cells from most of the donors. Given these results, LEA did not exhibit the desired therapeutic effect of ameliorating the deficit

in B-lymphoblast number, and further experimentation was discontinued. OEA, however, did demonstrate effects on cultured cells that would suggest a potential for benefit in the treatment of lymphopenia *in vivo*. Although OEA has not yet been reported in the literature as a therapeutic for BTHS, it has been considered as a therapeutic treatment option for other disorders. Indeed, numerous studies have highlighted the positive effects of OEA on intestinal inflammation [128], obesity [129], and non-alcoholic fatty liver disease [130]. This is however, the first time that OEA was shown to modulate B-lymphoblasts from BTHS patients. Thus, additional studies to better understand the mechanism underlying the increase in BTHS lymphoblast numbers are warranted.

The next objective of this thesis investigated the treatment effects of OEA on CL metabolism and the CL composition of BTHS and healthy lymphoblasts, to gain insight as to whether OEA may improve the rate of lymphoblast cell expansion by restoring CL defects caused by *TAZ* deficiency. Since previous reports have attributed detriments in the mitochondrial function and health of BTHS lymphoblasts directly to alterations of CL content and CL composition [52, 96], I hypothesized that the primary mechanism behind the effects of OEA on BTHS lymphoblast expansion was an increase in CL content, or a restoration of the CL fatty acyl profile, to more closely match healthy controls. While results from my study did show an effect of OEA on the mRNA expression level in BTHS lymphoblasts of three genes involved in CL synthesis, OEA surprisingly had minimal effects on either CL content or composition. As the current data only has a single biological replicate, it is important to note that analysis of the cardiolipin fatty acyl composition and content of additional BTHS and healthy lymphoblast donors is needed, before any definitive conclusion can be drawn. However, since lymphoblasts from every BTHS donor responded positively to OEA, it is notable that in at least one

respondant donor cell set, this was not associated with significant changes to CL. Thus, this work suggests that other factors should be examined in greater detail.

Apart from the detriments in mitochondrial CL, evidence suggests that other membrane phospholipids seem to be affected by BTHS as well [131]. This is highlighted in a recent report that showed a decrease in membrane plasmalogen levels in several BTHS tissue types, including human lymphoblasts, mouse brain tissue, mouse liver, and mouse kidney [131]. Since plasmalogens are membrane phospholipids previously shown to have antioxidation effects [132, 133], an increase in plasmalogen levels may help to decrease the build up of ROS from dysfunctional mitochondria in BTHS lymphoblasts, thus maintaining the mitochondrial membrane potential and preventing cell death. While the effects of OEA on plasmalogen biosynthesis are not fully understood in the literature, the addition of an ethanolamine head group onto 1-0-alkyl-2-acyl-*sn*-glycerol is an important step in the biosynthesis of a specific type of plasmalogen (plasmenylethanolamine) [133]. Hence, it is possible that the endogenous treatment of oleylethanolamine (OEA) could potentially increase the availability of free ethanolamine to promote plasmalogen biosynthesis. Nonetheless, future studies could aim to examine plasmalogen content using mass spectrometry in BTHS cells following OEA treatment.

Another possible factor that may explain the effects of OEA on the promotion of BTHS lymphocyte number expansion involves the mitochondrial glycerophospholipid, PE. Specifically, PE accounts for up to 25% of the total phospholipids in the inner mitochondrial membrane, and has been shown to be vital for the stability and function of the electron transport chain and the formation of the mitochondrial cristae structure [134, 135]. Similar to plasmalogens, it is possible that the treatment with OEA may promote the biosynthesis of PE via the Kennedy pathway, by providing an increased availability of ethanolamine [136]. This may contribute to a

better overall mitochondrial function in BTHS lymphoblasts, leading to reduced cell death and greater proliferative capacity. For this reason, future experimenters could also analyze the total PE content in BTHS lymphoblast, to determine if the treatment of OEA will significantly increase this phospholipid group.

Finally, instead of promoting the increase in plasmalogen and PE biosynthesis, free ethanolamine has also been shown previously to exhibit growth-stimulatory effects when cultured with mammalian cells [136]. This was demonstrated in a study using a rat animal model, where the treatment with ethanolamine increased the cell proliferation rate of hepatocytes both *in vivo* and *in vitro* [137]. Additionally, ethanolamine has also been shown to enhance the proliferative capacity of epithelial cells, through an increase in mitochondrial function and mTOR signalling [138]. Therefore, an increase in lymphoblast growth might be mediated by an increase in ethanolamine influx from OEA, which contributes to an increase in lymphoblast proliferation.

Other more direct explanations for the beneficial effects of OEA in this work, beyond non-specific stimulatory events occurring downstream of ethanolamine provision, should also be considered, given that OEA is a receptor agonist for PPAR α and TRPV1, which have both been shown previously to modulate mitochondrial function [111, 121]. Results from this thesis suggest that the effect of OEA on BTHS lymphoblast cell number increases could instead be caused by the direct modulation of the mitochondria. This possible mechanism gave rise to the experiments described in the final objective of this thesis, which analyzed differences in mitochondrial shape, number, size, and cristae length between healthy and BTHS lymphoblasts treated with OEA or vehicle. Surprisingly, OEA increased the mitochondrial number, while simultaneously decreasing the total mitochondrial size, in two distinct BTHS lymphoblast

donors. Based on thesis findings, I theorized that the effect of OEA was likely caused by the induction or activation of DRP1 to facilitate mitochondrial fission, which would be expected to promote both mitophagy and lymphoblast proliferation. Alternatively, OEA may also increase the expression of PGC1- α to increase mitochondrial biogenesis, which would either decrease ROS-induced lymphoblast cell death, or promote lymphoblast proliferation, and either effect (or a combination) could explain the effects observed on lymphoblast number expansion.

While the proposed effects of OEA to activate mitochondrial biogenesis and mitochondrial fission sounds reasonable, it is still unclear whether or not mitochondrial biogenesis and fission are activated co-committedly, or if only one process is activated. For example, the induction of mitochondrial fission and biogenesis could both lead to an increase in mitochondrial number in a TEM analysis [139, 140]. However, since only mitochondrial biogenesis can lead to an expansion of the mitochondrial volume (mass) [140], an additional analysis using mitochondrial density may provide greater insights on the mechanism behind the effects of OEA treatment. As such, an increase in mitochondrial density and number, with a concomitant decrease in mitochondrial size, would likely indicate that both fission and biogenesis are simultaneously activated. Whereas, if mitochondrial density decreases or remains the same, while mitochondrial size decreases and mitochondrial number increases, this would indicate that only fission is activated.

Given these assumptions, additional mitochondrial density measurements of BTHS and healthy lymphoblasts treated with or without OEA were analyzed and compared. Results from this analysis suggest that OEA treatment did not elicit a major change in the mitochondrial density of BTHS individuals (**Fig. 10**). This might indicate that mitochondrial biogenesis is not the primary mechanism underlying the effects of OEA on BTHS lymphoblasts. However, since

this analysis is purely just an observation based on the TEM images from two individual sets of BTHS and healthy donors, future studies should focus on the quantifications of proteins levels of DRP1 and PGC-1 α in both OEA- and vehicle-treated BTHS lymphoblasts, which will provide greater insight into the effects of OEA on mitochondrial fission and biogenesis. As well, quantifying the number of cells undergoing mitophagy, autophagy, and necrosis between OEA and vehicle treated BTHS lymphoblasts will confirm if OEA will decrease BTHS lymphoblast death. Finally, a cell cycle analysis will help to determine the differences in proliferation capacity between OEA- and vehicle-treated BTHS lymphoblasts.

This thesis has several limitations. Thesis study II only tested a single BTHS and healthy lymphoblast set for the analysis of CL content and composition. This is problematic, as individual BTHS donors may respond differently to OEA treatment, meaning that the observed effects of OEA on CL content and composition of a single BTHS and healthy lymphoblast set might not reflect the results of a cohort of BTHS patients. Another limitation pertains to the premature discontinuation of further LEA studies in thesis II and III. This decision was due to resource limitations, so I only pursued treatment that had an initial beneficial effect on BTHS cell number, because lymphopenia was the primary therapeutic outcome. With more resources, it would have been interesting to compare the differences in mitochondrial number and size between LEA- and OEA- treated BTHS lymphoblast, which might have helped to provide insight into the lack of effect of LEA on BTHS lymphoblasts. Additionally, this could also provide evidence to help explain differential effects of OEA on BTHS lymphoblasts, as well. The final critique relates to the study design of this experiment. Since studies were performed *in vitro*, this means the effects of OEA and LEA were observed in ideal experimental conditions, void of confounding variables. While cultured cells are cheaper and more readily available

compared to animal models, determination of the effects of OEA and LEA on *Taz*-deficient mice would be much more relevant to humans than cell treatments. Additionally, an *in vivo* approach will also help identify any potential side effects of treatments, as well.

Despite the limitations, this study is not without its strengths. First, the use of double blinding for the cell counts of the first two sets of BTHS and healthy lymphoblast (AG15022 & GM22192, AG14947 & GM22193) ensured that the effect of OEA on BTHS lymphoblast number were true effects and not due to confirmation bias. Another important strength is the novelty of this research. To the best of my knowledge this was the first study of its kind to use NAE as a therapeutic agent for the treatment of BTHS. Additionally, this thesis also used a wide variety of analytical techniques, including transmission electron microscopy (TEM), quantitative polymerase chain reaction (qPCR), and gas chromatography (GC), which provided great insights on the potential mechanisms behind the effects of OEA on BTHS lymphoblast. Finally, a major confounding variable was removed with the use of charcoal stripped FBS. This ensured that the effects of NAE treatment were not due to residual bioactive lipids within the media.

Although OEA was found to improve the expansion of BTHS lymphoblast cultures, as well as mitochondrial morphology, it is important to carefully consider whether this compound should be pursued as a therapeutic strategy for the treatment of BTHS in humans. OEA was shown to rescue the deficit in total cell number of cultured BTHS lymphoblasts, which suggest that its use in BTHS patients might lead to an improvement in the adaptive immune system. However, the rescue of cell number was only partial, and did not reach levels of healthy controls, even after four full days of administration. This may be due to the fact that OEA had little effect on BTHS CL content and composition, and therefore it is unlikely to repair the underlying cristae abnormalities. For a full rescue effect to occur, the proposed therapeutic agent will not only need

to increase the endogenous production of CL, but also promote the remodelling of MLCL and DLCL back to mature CL with a fatty acyl profile that matches healthy controls. There are further practical limitations to the use of OEA as a therapeutic. Some of the downstream receptors of OEA (*i.e.* GPR119, PPAR α and TRPV1) have been shown to increase satiety and reduce feeding in animal models [71, 74]. This means that the treatment with OEA in BTHS patients will lead to reduced eating, which might exacerbate the already prominent symptoms of growth delay and skeletal myopathy apparent in patients with this disorder.

In conclusion, taking into the consideration of the potential side effects of OEA, and the incomplete rescue of BTHS lymphoblasts, OEA is not an ideal candidate as a therapeutic modulator of BTHS syndrome and its treatment should not be recommended in BTHS patients exhibiting symptoms of skeletal myopathy and major growth delays. Additionally, due to the lack of observed effects of LEA on lymphoblast number, it is suggested that LEA is also not an ideal therapeutic candidate for BTHS. Nevertheless, this study provided novel insights on the efficacy of OEA and LEA as therapeutic modulators of BTHS, which will provide an avenue for future researchers to examine the use other NAE species or compounds for the treatment of BTHS syndrome.

Table 4: Summary of key findings

Thesis Study I: Effects of OEA and LEA on BTHS and control lymphoblast cell number	
Key findings	<ul style="list-style-type: none"> • Following four days of culturing, BTHS lymphoblast had significantly less total cell number compared to healthy controls. • OEA partially restored the deficit in cell number of BTHS lymphoblasts, but the increase did not reach healthy control levels after four days of growth. • LEA had no significant effects on the cell number of BTHS lymphoblast
Thesis Study II: Effects of OEA on CL metabolism and composition	
Key findings	<ul style="list-style-type: none"> • BTHS lymphoblasts have higher mRNA expression levels of <i>PGPS</i>, <i>CDS1</i>, and <i>GPAT3</i>. • Treatment with OEA normalized the expression levels of <i>PGPS</i>, <i>CDS1</i>, and <i>GPAT</i>, so that they were closer to healthy controls. • OEA treatment slightly decreased the CL content of one BTHS lymphoblast donor. • OEA treatment of BTHS lymphoblast did not alter the relative content of individual fatty acid in CL
Thesis Study III: Effect of OEA on BTHS lymphoblast Mitochondria number, size, and morphology	
Key findings	<ul style="list-style-type: none"> • BTHS lymphoblasts have decreased parallel cristae, greater mitochondrial size compared to healthy controls. • OEA treatment increase the mitochondrial number and decreased the mitochondrial size of BTHS lymphoblast • Decreased ratio of giant mitochondria in BTHS lymphoblasts following OEA treatment.

References

1. Dudek, J. and C. Maack, *Barth syndrome cardiomyopathy*. Cardiovasc Res, 2017.
2. Barth, P.G., Scholte, H.R., Berden, J.A., Van der Klei-Van Moorsel, J.M., Luyt-Houwen, I.E., Van 't Veer-Korthof, E.T., Van der Harten, J.J., Sobotka-Plojhar, M.A., *An X-linked mitochondrial disease affecting cardiac muscle, skeletal muscle and neutrophil leucocytes*. J Neurol Sci, 1983. **62**(1-3): p. 327-55.
3. Gonzalez, I.L. *Human tafazzin (TAZ) gene mutation and variation database*. 2012. Science and Research section of <http://www.barthsyndrome.org>.:[
4. Acehan, D., et al., *Cardiac and skeletal muscle defects in a mouse model of human Barth syndrome*. J Biol Chem, 2011. **286**(2): p. 899-908.
5. Schlame, M. and M. Ren, *Barth syndrome, a human disorder of cardiolipin metabolism*. FEBS Lett, 2006. **580**(23): p. 5450-5.
6. Roberts, A.E., et al., *The Barth Syndrome Registry: distinguishing disease characteristics and growth data from a longitudinal study*. Am J Med Genet A, 2012. **158A**(11): p. 2726-32.
7. Clarke, S.L., Bowron, A., Gonzalez, I. L., Groves, S. J., Newbury-Ecob, R., Clayton, N., ... Steward, C. G., *Barth syndrome*. Orphanet journal of rare diseases, 2013. **8**(23).
8. Steward, C.G., et al., *Neutropenia in Barth syndrome: characteristics, risks, and management*. Curr Opin Hematol, 2019. **26**(1): p. 6-15.
9. van Raam, B.J. and T.W. Kuijpers, *Mitochondrial defects lie at the basis of neutropenia in Barth syndrome*. Curr Opin Hematol, 2009. **16**(1): p. 14-9.
10. Kuijpers, T.W., et al., *Neutrophils in Barth syndrome (BTHS) avidly bind annexin-V in the absence of apoptosis*. Blood, 2004. **103**(10): p. 3915-23.
11. Makaryan, V., et al., *The cellular and molecular mechanisms for neutropenia in Barth syndrome*. Eur J Haematol, 2012. **88**(3): p. 195-209.
12. Finsterer, J. and M. Frank, *Haematological features in Barth syndrome*. Curr Opin Hematol, 2013. **20**(1): p. 36-40.
13. Skyes, D. *Neutropenia in Barth Syndrome: Endoplasmic reticulum stress and an increased sensitivity to apoptosis*. in 2020 BSF Scientific and Medical Symposium 2020. Barth Syndrome Foundation

14. Corrado, M. *Dynamic cardiolipin synthesis and remodeling is required for CD8+ T cell immunity*. in *2020 BSF Scientific and Medical Symposium 2020*. Barth Syndrome Foundation.
15. Institute, C. *LCL from B-lymphocytes*. 2020; Available from: https://www.coriell.org/0/sections/Search/Sample_Detail.aspx?Ref=GM12892&product=C
[C](#).
16. Pangborn, M.C., *Isolation and purification of a serologically active phospholipid from beef heart*. *J Biol Chem*, 1942. **247**(56).
17. Hatch, G.M., *Cell biology of cardiac mitochondrial phospholipids*. *Biochem Cell Biol*, 2004. **82**(1): p. 99-112.
18. McMillin, J.B., Dowhan, W., *Cardiolipin and apoptosis*. *Biochim Biophys Acta*, 2002. **1585**(2-3): p. 97-107.
19. Paradies, G., et al., *Functional role of cardiolipin in mitochondrial bioenergetics*. *Biochim Biophys Acta*, 2014. **1837**(4): p. 408-17.
20. Scorrano, L., *Caspase-8 goes cardiolipin: a new platform to provide mitochondria with microdomains of apoptotic signals?* *J Cell Biol*, 2008. **183**(4): p. 579-81.
21. Ellis, C.E., et al., *Mitochondrial lipid abnormality and electron transport chain impairment in mice lacking alpha-synuclein*. *Mol Cell Biol*, 2005. **25**(22): p. 10190-201.
22. Dolinsky, V.W., et al., *Cardiac mitochondrial energy metabolism in heart failure: Role of cardiolipin and sirtuins*. *Biochim Biophys Acta*, 2016. **1861**(10): p. 1544-54.
23. Shi, Y., *Emerging roles of cardiolipin remodeling in mitochondrial dysfunction associated with diabetes, obesity, and cardiovascular diseases*. *J Biomed Res*, 2010. **24**(1): p. 6-15.
24. Vreken, P., et al., *Defective remodeling of cardiolipin and phosphatidylglycerol in Barth syndrome*. *Biochem Biophys Res Commun*, 2000. **279**(2): p. 378-82.
25. Sapandowski, A., et al., *Cardiolipin composition correlates with prostate cancer cell proliferation*. *Mol Cell Biochem*, 2015. **410**(1-2): p. 175-85.
26. Zhang, J., et al., *Cardiolipins Are Biomarkers of Mitochondria-Rich Thyroid Oncocytic Tumors*. *Cancer Res*, 2016. **76**(22): p. 6588-6597.
27. Paradies, G., et al., *Oxidative stress, mitochondrial bioenergetics, and cardiolipin in aging*. *Free Radic Biol Med*, 2010. **48**(10): p. 1286-95.

28. Ikon, N. and R.O. Ryan, *Cardiolipin and mitochondrial cristae organization*. Biochim Biophys Acta Biomembr, 2017. **1859**(6): p. 1156-1163.
29. Schlame, M., *Cardiolipin synthesis for the assembly of bacterial and mitochondrial membranes*. J Lipid Res, 2008. **49**(8): p. 1607-20.
30. Paumard, P., Vaillier, J., Couлары, B., Schaeffer, J., Soubannier, V., Mueller, D. M., ... Velours, J. , *The ATP synthase is involved in generating mitochondrial cristae morphology*. The EMBO journal, 2002. **21**(3): p. 221-230.
31. Acehan, D., et al., *Cardiolipin affects the supramolecular organization of ATP synthase in mitochondria*. Biophys J, 2011. **100**(9): p. 2184-92.
32. Petrosillo, G., et al., *Mitochondrial dysfunction in rat with nonalcoholic fatty liver Involvement of complex I, reactive oxygen species and cardiolipin*. Biochim Biophys Acta, 2007. **1767**(10): p. 1260-7.
33. Schwall, C.T., V.L. Greenwood, and N.N. Alder, *The stability and activity of respiratory Complex II is cardiolipin-dependent*. Biochim Biophys Acta, 2012. **1817**(9): p. 1588-96.
34. Robinson, N.C., *Functional binding of cardiolipin to cytochrome c oxidase*. Journal of Bioenergetics and Biomembranes, 1993. **25**(2): p. 153-163.
35. Gomez, B., & Robinson, N. C., *Phospholipase Digestion of Bound Cardiolipin Reversibly Inactivates Bovine Cytochrome bc₁ l*. Biochemistry, 1999. **38**(28): p. 9031-9038.
36. Althoff, T., et al., *Arrangement of electron transport chain components in bovine mitochondrial supercomplex III_{IV}I*. EMBO J, 2011. **30**(22): p. 4652-64.
37. Kadenbach, B., Mende, P., Kolbe, H., Stipani, I., & Palmieri, F., *The mitochondrial phosphate carrier has an essential requirement for cardiolipin*. FEBS Letters, 1982. **139**(1): p. 109–112.
38. Musatov, A. and E. Sedlak, *Role of cardiolipin in stability of integral membrane proteins*. Biochimie, 2017. **142**: p. 102-111.
39. Chicco, A.J. and G.C. Sparagna, *Role of cardiolipin alterations in mitochondrial dysfunction and disease*. Am J Physiol Cell Physiol, 2007. **292**(1): p. C33-44.
40. Stepanyants, N., et al., *Cardiolipin's propensity for phase transition and its reorganization by dynamin-related protein 1 form a basis for mitochondrial membrane fission*. Mol Biol Cell, 2015. **26**(17): p. 3104-16.

41. Bustillo-Zabalbeitia, I., et al., *Specific interaction with cardiolipin triggers functional activation of Dynamin-Related Protein 1*. PLoS One, 2014. **9**(7): p. e102738.
42. Ban, T., et al., *Molecular basis of selective mitochondrial fusion by heterotypic action between OPA1 and cardiolipin*. Nat Cell Biol, 2017. **19**(7): p. 856-863.
43. Liu, R. and D.C. Chan, *OPA1 and cardiolipin team up for mitochondrial fusion*. Nat Cell Biol, 2017. **19**(7): p. 760-762.
44. Youle, R.J. and A.M. van der Bliek, *Mitochondrial fission, fusion, and stress*. Science, 2012. **337**(6098): p. 1062-5.
45. Anton, Z., et al., *Human Atg8-cardiolipin interactions in mitophagy: Specific properties of LC3B, GABARAPL2 and GABARAP*. Autophagy, 2016. **12**(12): p. 2386-2403.
46. Gonzalvez, F., et al., *Cardiolipin provides an essential activating platform for caspase-8 on mitochondria*. J Cell Biol, 2008. **183**(4): p. 681-96.
47. Lutter, M., Fang, M., Luo, X., Nishijima, M., Xie, X.-S., & Wang, X., *Cardiolipin provides specificity for targeting of tBid to mitochondria*. Nature Cell Biology. **2**(10): p. 754-756.
48. Kantari, C. and H. Walczak, *Caspase-8 and bid: caught in the act between death receptors and mitochondria*. Biochim Biophys Acta, 2011. **1813**(4): p. 558-63.
49. Lai, Y.C., et al., *The role of cardiolipin in promoting the membrane pore-forming activity of BAX oligomers*. Biochim Biophys Acta Biomembr, 2019. **1861**(1): p. 268-280.
50. Mejia, E.M., H. Nguyen, and G.M. Hatch, *Mammalian cardiolipin biosynthesis*. Chem Phys Lipids, 2014. **179**: p. 11-6.
51. Rocquelin, G., Guenot, L., Astorg, P.O., David, M., *Phospholipid content and fatty acid composition of human heart*. Lipids, 1989. **24**(9): p. 775-80.
52. Xu, Y., et al., *Characterization of lymphoblast mitochondria from patients with Barth syndrome*. Lab Invest, 2005. **85**(6): p. 823-30.
53. Houtkooper, R.H., et al., *Identification and characterization of human cardiolipin synthase*. FEBS Lett, 2006. **580**(13): p. 3059-64.
54. Ye, C., Z. Shen, and M.L. Greenberg, *Cardiolipin remodeling: a regulatory hub for modulating cardiolipin metabolism and function*. J Bioenerg Biomembr, 2016. **48**(2): p. 113-23.
55. Xu, Y., et al., *The enzymatic function of tafazzin*. J Biol Chem, 2006. **281**(51): p. 39217-24.

56. Field, C.J., et al., *Human health benefits of vaccenic acid*. Appl Physiol Nutr Metab, 2009. **34**(5): p. 979-91.
57. Precht D, M.J., *C18:1, C18:2 and C18:3 trans and cis fatty acid isomers including conjugated cis delta 9, trans delta 11 linoleic acid (CLA) as well as total fat composition of German human milk lipids*. Nahrung, 1999. **43**(4): p. 233-244.
58. Matsuzaka, T. and H. Shimano, *Elovl6: a new player in fatty acid metabolism and insulin sensitivity*. J Mol Med (Berl), 2009. **87**(4): p. 379-84.
59. Blewett, H.J., et al., *Vaccenic acid favourably alters immune function in obese JCR:LA-cp rats*. Br J Nutr, 2009. **102**(4): p. 526-36.
60. Helioswilton Sales-Campos, P.R.d.S., Bethanea Crema Peghini, Joao Santana da Silva and Cristina Ribeiro Cardoso, *An Overview of the Modulatory Effects of Oleic Acid in Health and Disease*”, *Mini-Reviews in Medicinal Chemistry*. Mini-Reviews in Medicinal Chemistry, 2013. **13**(201).
61. Vick, J.F.M.D.C.Z.B.A., *Genetic Control of High Oleic Acid Content in Sunflower Oil*. Crop Science, 1987. **27**(5).
62. Paton, C.M., & Ntambi, J. M. , *Biochemical and physiological function of stearyl-CoA desaturase*. American journal of physiology. Endocrinology and metabolism. 2009. **297**(1): p. E28–E37.
63. Ting, H.C., et al., *Double bonds of unsaturated fatty acids differentially regulate mitochondrial cardiolipin remodeling*. Lipids Health Dis, 2019. **18**(1): p. 53.
64. Moussa, M., et al., *Relationship between the fatty acid composition of rat lymphocytes and immune functions*. Br J Nutr, 2000. **83**(3): p. 327-33.
65. Frigolet, M.E. and R. Gutierrez-Aguilar, *The Role of the Novel Lipokine Palmitoleic Acid in Health and Disease*. Adv Nutr, 2017. **8**(1): p. 173S-181S.
66. Murke, E., et al., *The mitochondrial phospholipid cardiolipin is involved in the regulation of T-cell proliferation*. Biochim Biophys Acta, 2016. **1861**(8 Pt A): p. 748-54.
67. Whelan, J. and K. Fritsche, *Linoleic acid*. Adv Nutr, 2013. **4**(3): p. 311-2.
68. Acehan, D., et al., *Comparison of lymphoblast mitochondria from normal subjects and patients with Barth syndrome using electron microscopic tomography*. Lab Invest, 2007. **87**(1): p. 40-8.

69. Ueda, N., K. Tsuboi, and T. Uyama, *N-acylethanolamine metabolism with special reference to N-acylethanolamine-hydrolyzing acid amidase (NAAA)*. *Prog Lipid Res*, 2010. **49**(4): p. 299-315.
70. Kaczocha, M., et al., *Fatty acid binding protein deletion suppresses inflammatory pain through endocannabinoid/N-acylethanolamine-dependent mechanisms*. *Mol Pain*, 2015. **11**: p. 52.
71. Tsuboi, K., et al., *Endocannabinoids and related N-acylethanolamines: biological activities and metabolism*. *Inflamm Regen*, 2018. **38**: p. 28.
72. Fu, J., et al., *Oleylethanolamide regulates feeding and body weight through activation of the nuclear receptor PPAR-alpha*. *Nature*, 2003. **425**(6953): p. 90-3.
73. Ashton, C.H. and P.B. Moore, *Endocannabinoid system dysfunction in mood and related disorders*. *Acta Psychiatr Scand*, 2011. **124**(4): p. 250-61.
74. Hansen, H.S. and T.A. Diep, *N-acylethanolamines, anandamide and food intake*. *Biochem Pharmacol*, 2009. **78**(6): p. 553-60.
75. Scherma, M., et al., *Brain activity of anandamide: a rewarding bliss?* *Acta Pharmacol Sin*, 2019. **40**(3): p. 309-323.
76. Lu, H.C. and K. Mackie, *An Introduction to the Endogenous Cannabinoid System*. *Biol Psychiatry*, 2016. **79**(7): p. 516-25.
77. Romano, A., et al., *Oleylethanolamide: a novel potential pharmacological alternative to cannabinoid antagonists for the control of appetite*. *Biomed Res Int*, 2014. **2014**: p. 203425.
78. Overton, H.A., M.C. Fyfe, and C. Reynet, *GPR119, a novel G protein-coupled receptor target for the treatment of type 2 diabetes and obesity*. *Br J Pharmacol*, 2008. **153 Suppl 1**: p. S76-81.
79. Artmann, A., et al., *Influence of dietary fatty acids on endocannabinoid and N-acylethanolamine levels in rat brain, liver and small intestine*. *Biochim Biophys Acta*, 2008. **1781**(4): p. 200-12.
80. Ishida, T., et al., *Linoleoyl ethanolamide reduces lipopolysaccharide-induced inflammation in macrophages and ameliorates 2,4-dinitrofluorobenzene-induced contact dermatitis in mice*. *Eur J Pharmacol*, 2013. **699**(1-3): p. 6-13.

81. Raboune, S., et al., *Novel endogenous N-acyl amides activate TRPV1-4 receptors, BV-2 microglia, and are regulated in brain in an acute model of inflammation*. Front Cell Neurosci, 2014. **8**: p. 195.
82. Wang, X., Chen, Y., Jin, Q., Huang, J., & Wang, X., *Synthesis of Linoleoyl Ethanolamide* J Oleo Science 2013. **62**((6)): p. 427-433.
83. Sun, Y.X., Tsuboi, K., Okamoto, Y., Tonai, T., Murakami, M., Kudo, I., & Ueda, N., *Biosynthesis of anandamide and N-palmitoylethanolamine by sequential actions of phospholipase A2 and lysophospholipase D*. The Biochemical journal, 2004. **380**(pt 3): p. 749-756.
84. Uyama, T., et al., *Involvement of phospholipase A/acyltransferase-1 in N-acylphosphatidylethanolamine generation*. Biochim Biophys Acta, 2013. **1831**(12): p. 1690-701.
85. Bradley, R.M., *Identification and characterization of a novel microsomal enzyme involved in cardiolipin synthesis and remodeling in Kinesiology* 2018, University of Waterloo Waterloo. p. 157.
86. Pecze, L., et al., *Endogenous TRPV1 stimulation leads to the activation of the inositol phospholipid pathway necessary for sustained Ca(2+) oscillations*. Biochim Biophys Acta, 2016. **1863**(12): p. 2905-2915.
87. Lee, S.S.T., et al., *Requirement of PPAR α in maintaining phospholipid and triacylglycerol homeostasis during energy deprivation*. J Lipid Res, 2004. **45**: p. 2025-2037.
88. Webster, J., Jiang, J. Y., Lu, B., Xu, F. Y., Taylor, W. A., Mymin, M., Zhang, M., Minuk, G. Y., & Hatch, G. M. , *On the mechanism of the increase in cardiolipin biosynthesis and resynthesis in hepatocytes during rat liver regeneration*. The Biochemical journal, 2005. **386**((part 1)): p. 137-143.
89. Jiang, Y.J., et al., *Stimulation of cardiac cardiolipin biosynthesis by PPAR α activation*. J Lipid Res, 2004. **45**(2): p. 244-52.
90. Cabral, G.A. and L. Griffin-Thomas, *Emerging role of the cannabinoid receptor CB2 in immune regulation: therapeutic prospects for neuroinflammation*. Expert Rev Mol Med, 2009. **11**: p. e3.

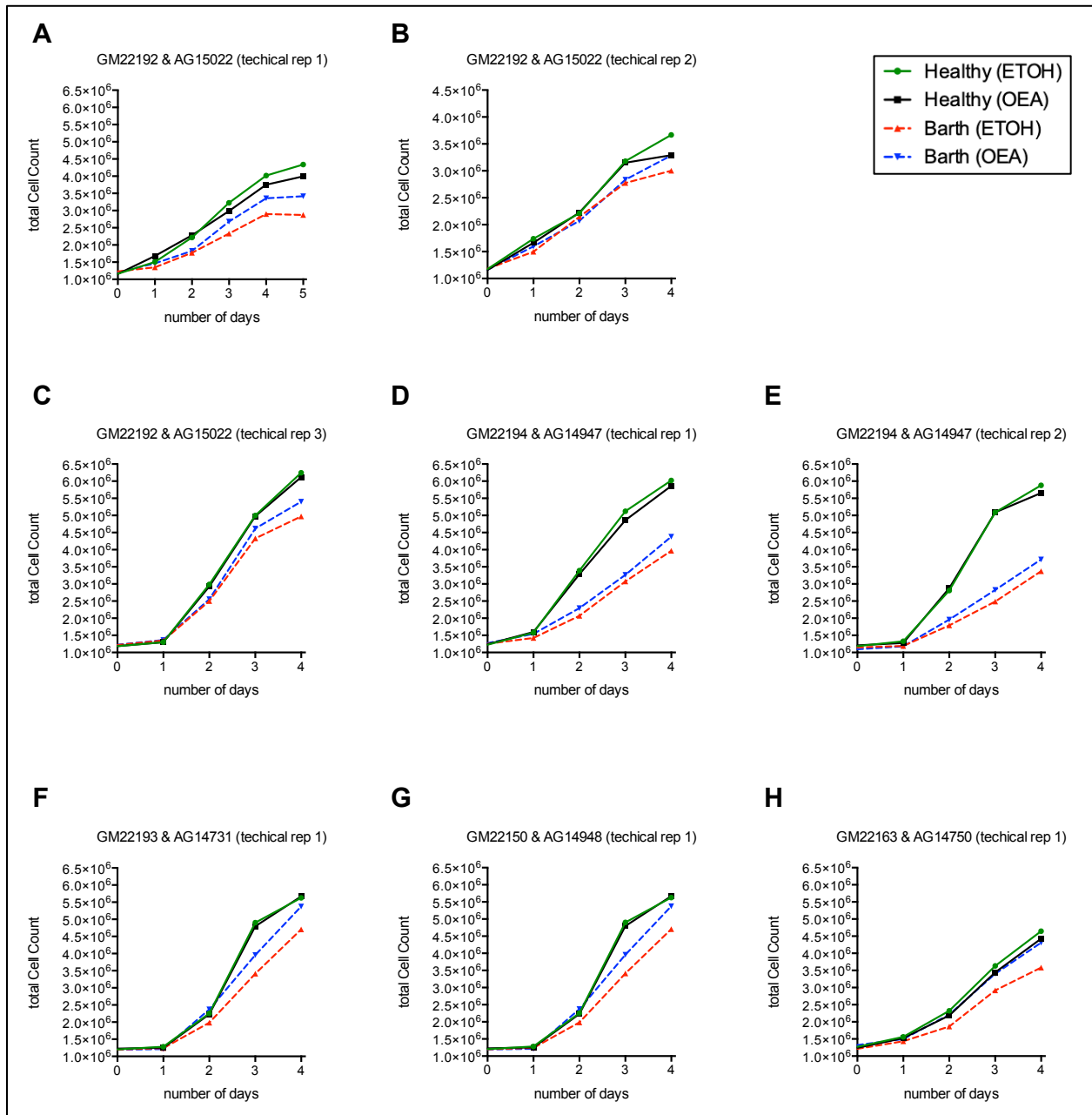
91. Alharthi, N., et al., *n-3 polyunsaturated N-acyl ethanolamines are CB2 cannabinoid receptor-preferring endocannabinoids*. *Biochim Biophys Acta Mol Cell Biol Lipids*, 2018. **1863**(11): p. 1433-1440.
92. Bione S, D.P., Maestrini E, Gedeon AK, Bolhuis PA, Toniolo D, *A novel X-linked gene, G4.5, is responsible for Barth syndrome*. *Nature Genetics*, 1996. **12**: p. 385-389.
93. Pfeiffer, K., et al., *Cardiolipin stabilizes respiratory chain supercomplexes*. *J Biol Chem*, 2003. **278**(52): p. 52873-80.
94. Paradies, G., et al., *Role of Cardiolipin in Mitochondrial Function and Dynamics in Health and Disease: Molecular and Pharmacological Aspects*. *Cells*, 2019. **8**(7).
95. Institute, C. *Catalog items 2019*; Available from: <https://www.coriell.org/Search?q=%22BARTH%20SYNDROME%22>.
96. Gonzalvez, F., et al., *Barth syndrome: cellular compensation of mitochondrial dysfunction and apoptosis inhibition due to changes in cardiolipin remodeling linked to tafazzin (TAZ) gene mutation*. *Biochim Biophys Acta*, 2013. **1832**(8): p. 1194-206.
97. Rigaud C, L.A., Touraine R, et al., *Natural history of Barth syndrome: a national cohort study of 22 patients*. *Orphanet J Rare Dis*, 2013. **8**(70).
98. Basu, S. and B.N. Dittel, *Unraveling the complexities of cannabinoid receptor 2 (CB2) immune regulation in health and disease*. *Immunol Res*, 2011. **51**(1): p. 26-38.
99. ThermoFisher. *Counting Cells in a Hemocytometer*. n.d; Available from: <https://www.thermofisher.com/us/en/home/references/gibco-cell-culture-basics/cell-culture-protocols/counting-cells-in-a-hemocytometer.html>.
100. Ullman, E., et al., *Autophagy promotes necrosis in apoptosis-deficient cells in response to ER stress*. *Cell Death Differ*, 2008. **15**(2): p. 422-5.
101. Nikolettou, V., et al., *Crosstalk between apoptosis, necrosis and autophagy*. *Biochim Biophys Acta*, 2013. **1833**(12): p. 3448-3459.
102. Mandal, S., et al., *Mitochondrial function controls proliferation and early differentiation potential of embryonic stem cells*. *Stem Cells*, 2011. **29**(3): p. 486-95.
103. Invitrogen. *TRIZOL Reagent*. 2016; Available from: http://tools.thermofisher.com/content/sfs/manuals/trizol_reagent.pdf.
104. ThermoFisher. *High Capacity cDNA Reverse Transcription Kit* 2018; Available from: <https://www.thermofisher.com/document-connect/document->

- [connect.html?url=https://assets.thermofisher.com/TFS-Assets/LSG/manuals/MAN0017977_highcap_cDNA_RT_UG.pdf&title=VXNlciBHdWlkZTogSGlnaCBDYXBhY2l0eSBjRE5BIFJldmVyc2UgVHJhbnNjcmlwdGlvbiBLaXQ=&fbclid=IwAR1pKT4VVcgGAibo36b6m1ZNfwFmrcfkIVHCaDxbjM8twmS4P4dVbI9alM4](https://assets.thermofisher.com/TFS-Assets/LSG/manuals/MAN0017977_highcap_cDNA_RT_UG.pdf&title=VXNlciBHdWlkZTogSGlnaCBDYXBhY2l0eSBjRE5BIFJldmVyc2UgVHJhbnNjcmlwdGlvbiBLaXQ=&fbclid=IwAR1pKT4VVcgGAibo36b6m1ZNfwFmrcfkIVHCaDxbjM8twmS4P4dVbI9alM4)
105. Schmittgen, T.D. and K.J. Livak, *Analyzing real-time PCR data by the comparative C(T) method*. Nat Protoc, 2008. **3**(6): p. 1101-8.
 106. Bradley, R.M., et al., *Lpaatdelta/Agpat4 deficiency impairs maximal force contractility in soleus and alters fibre type in extensor digitorum longus muscle*. Biochim Biophys Acta Mol Cell Biol Lipids, 2018. **1863**(7): p. 700-711.
 107. FOLCH, J., LEES, M., SLOANE STANLEY, G.H., *A simple method for the isolation and purification of total lipides from animal tissues*. J Biol Chem, 1957. **226**(1): p. 497-509.
 108. Chalil, A., et al., *PEMT, Delta6 desaturase, and palmitoyldocosahexaenoyl phosphatidylcholine are increased in rats during pregnancy*. J Lipid Res, 2018. **59**(1): p. 123-136.
 109. Stark, K.D.N.S., Jr., *Fast gas chromatography for the identification of fatty acid methyl esters from mammalian samples* Lipid Technol., 2005. **17**: p. 181-185.
 110. Chiang, H., et al., *Mitochondrial fission augments capsaicin-induced axonal degeneration*. Acta Neuropathol, 2015. **129**(1): p. 81-96.
 111. Huang, Y., et al., *The PPAR pan-agonist bezafibrate ameliorates cardiomyopathy in a mouse model of Barth syndrome*. Orphanet J Rare Dis, 2017. **12**(1): p. 49.
 112. Kroemer, G., Reed, J, *Mitochondrial control of cell death*. Nat Med, 2000. **6**: p. 513-519.
 113. Douiev, L., et al., *Bezafibrate Improves Mitochondrial Fission and Function in DNML-Deficient Patient Cells*. Cells, 2020. **9**(2).
 114. Mishra, P. and D.C. Chan, *Mitochondrial dynamics and inheritance during cell division, development and disease*. Nat Rev Mol Cell Biol, 2014. **15**(10): p. 634-46.
 115. Simula, L., et al., *Drp1 Controls Effective T Cell Immune-Surveillance by Regulating T Cell Migration, Proliferation, and cMyc-Dependent Metabolic Reprogramming*. Cell Rep, 2018. **25**(11): p. 3059-3073 e10.
 116. Zhan, L., Cao, H., Wang, G., Lyu, Y., Sun, X., An, J., Wu, Z., Huang, Q., Liu, B., & Xing, J., *Drp1-mediated mitochondrial fission promotes cell proliferation through crosstalk of*

- p53 and NF- κ B pathways in hepatocellular carcinoma*. *Oncotarget*, 2016. **7**(40): p. 65001-65011.
117. Yin, M., et al., *Silencing Drp1 inhibits glioma cells proliferation and invasion by RHOA/ROCK1 pathway*. *Biochem Biophys Res Commun*, 2016. **478**(2): p. 663-8.
 118. Kitamura, S., et al., *Drp1 regulates mitochondrial morphology and cell proliferation in cutaneous squamous cell carcinoma*. *J Dermatol Sci*, 2017. **88**(3): p. 298-307.
 119. Twig, G. and O.S. Shirihai, *The interplay between mitochondrial dynamics and mitophagy*. *Antioxid Redox Signal*, 2011. **14**(10): p. 1939-51.
 120. Twig, G., et al., *Fission and selective fusion govern mitochondrial segregation and elimination by autophagy*. *EMBO J*, 2008. **27**(2): p. 433-46.
 121. Luo, Z., et al., *TRPV1 activation improves exercise endurance and energy metabolism through PGC-1alpha upregulation in mice*. *Cell Res*, 2012. **22**(3): p. 551-64.
 122. St-Pierre, J., et al., *Suppression of reactive oxygen species and neurodegeneration by the PGC-1 transcriptional coactivators*. *Cell*, 2006. **127**(2): p. 397-408.
 123. Rasbach, K.A. and R.G. Schnellmann, *PGC-1alpha over-expression promotes recovery from mitochondrial dysfunction and cell injury*. *Biochem Biophys Res Commun*, 2007. **355**(3): p. 734-9.
 124. Austin, S. and J. St-Pierre, *PGC1alpha and mitochondrial metabolism--emerging concepts and relevance in ageing and neurodegenerative disorders*. *J Cell Sci*, 2012. **125**(Pt 21): p. 4963-71.
 125. Demir, S., et al., *Neutrophil-lymphocyte ratio in patients with major depressive disorder undergoing no pharmacological therapy*. *Neuropsychiatr Dis Treat*, 2015. **11**: p. 2253-8.
 126. Hamad, H. and A. Mangla, *Lymphocytosis*. StatPearls. StatPearls Publishing, 2020.
 127. Bain, B.J., *Bone marrow aspiration*. *J Clin Pathol*, 2001. **54**: p. 657-663.
 128. Karwad, M.A., et al., *Oleylethanolamine and palmitoylethanolamine modulate intestinal permeability in vitro via TRPV1 and PPARalpha*. *FASEB J*, 2017. **31**(2): p. 469-481.
 129. Brown, J.D., E. Karimian Azari, and J.E. Ayala, *Oleylethanolamide: A fat ally in the fight against obesity*. *Physiol Behav*, 2017. **176**: p. 50-58.
 130. Tutunchi, H., et al., *The effects of oleylethanolamide, an endogenous PPAR-alpha agonist, on risk factors for NAFLD: A systematic review*. *Obes Rev*, 2019. **20**(7): p. 1057-1069.

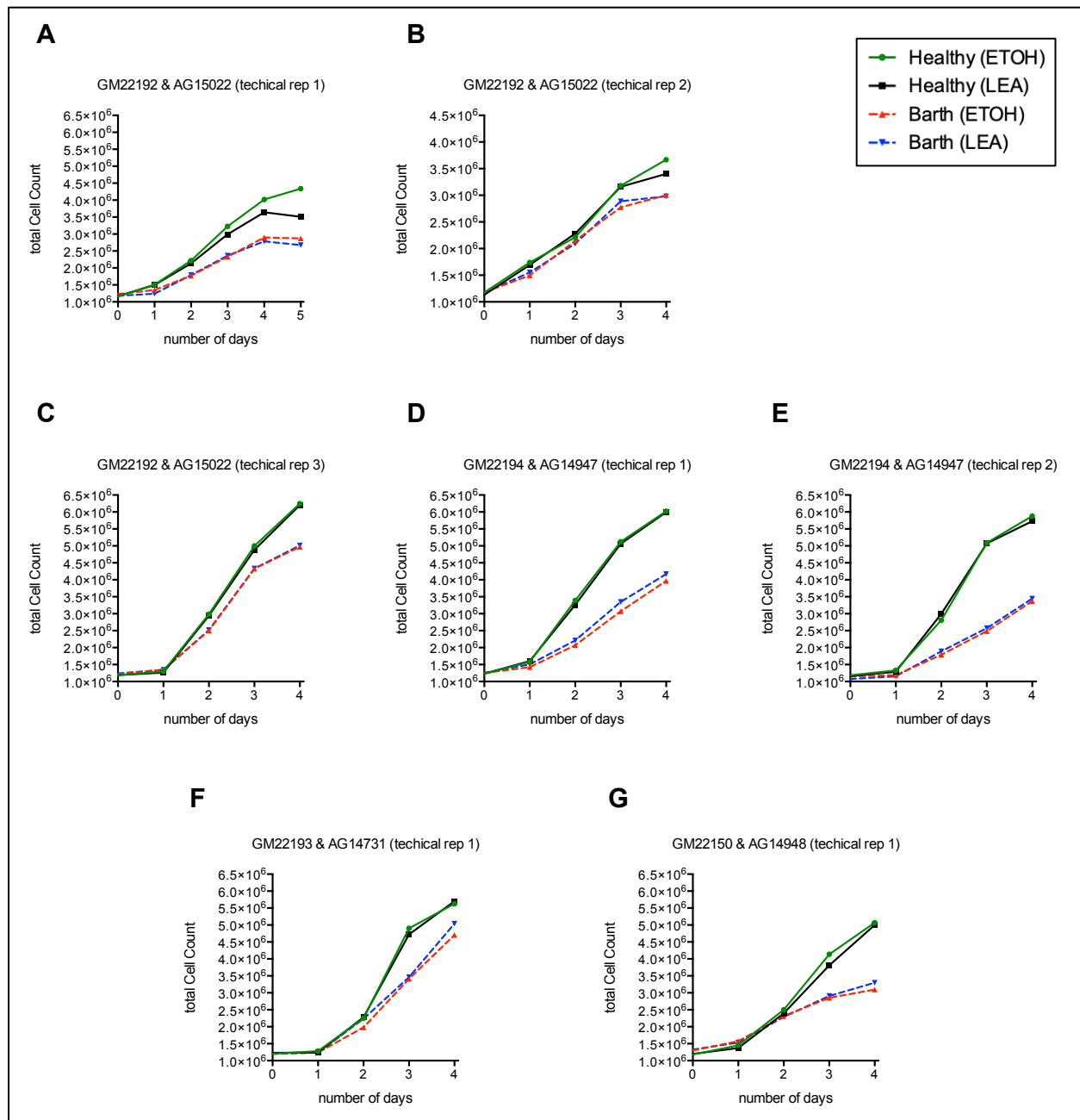
131. Kimura, T., et al., *Plasmalogen loss caused by remodeling deficiency in mitochondria*. Life Sci Alliance, 2019. **2**(4).
132. Kuczynski, B. and N.V. Reo, *Evidence that plasmalogen is protective against oxidative stress in the rat brain*. Neurochem Res, 2006. **31**(5): p. 639-56.
133. Braverman, N.E. and A.B. Moser, *Functions of plasmalogen lipids in health and disease*. Biochim Biophys Acta, 2012. **1822**(9): p. 1442-52.
134. Joshi, A.S., et al., *Cardiolipin and mitochondrial phosphatidylethanolamine have overlapping functions in mitochondrial fusion in Saccharomyces cerevisiae*. J Biol Chem, 2012. **287**(21): p. 17589-97.
135. Basu Ball, W., J.K. Neff, and V.M. Gohil, *The role of nonbilayer phospholipids in mitochondrial structure and function*. FEBS Lett, 2018. **592**(8): p. 1273-1290.
136. Patel, D. and S.N. Witt, *Ethanolamine and Phosphatidylethanolamine: Partners in Health and Disease*. Oxid Med Cell Longev, 2017. **2017**: p. 4829180.
137. Sasaki, H., et al., *Ethanolamine modulates the rate of rat hepatocyte proliferation in vitro and in vivo*. . Proceedings of the National Academy of Sciences of the United States of America, 1997. **94**(14): p. 7320-7325.
138. Yang, H., et al., *Ethanolamine enhances the proliferation of intestinal epithelial cells via the mTOR signaling pathway and mitochondrial function*. In Vitro Cell Dev Biol Anim, 2016. **52**(5): p. 562-7.
139. Scott, I. and R.J. Youle, *Mitochondrial fission and fusion*. Essays Biochem, 2010. **47**: p. 85-98.
140. Sanchis-Gomar, F., et al., *Mitochondrial biogenesis in health and disease. Molecular and therapeutic approaches*. Current pharmaceutical design, 2014. **20**(35): p. 5619-5633.

Appendices



Appendix figure 1: Technical replicates of the growth data of each individual BTHS and healthy lymphoblast donors, treated with OEA or vehicle.

(A-C) represents technical reps of GM22192 (BTHS) & AG15022 (healthy), (D-E) represents technical reps of GM22194 (BTHS) & AG14947 (healthy), (F-H) represents a single technical rep of GM22193 (BTHS) & AG14731 (healthy), GM22150 (BTHS) & AG14948 (healthy), and GM22163 (BTHS) & AG14750 (healthy), respectively.

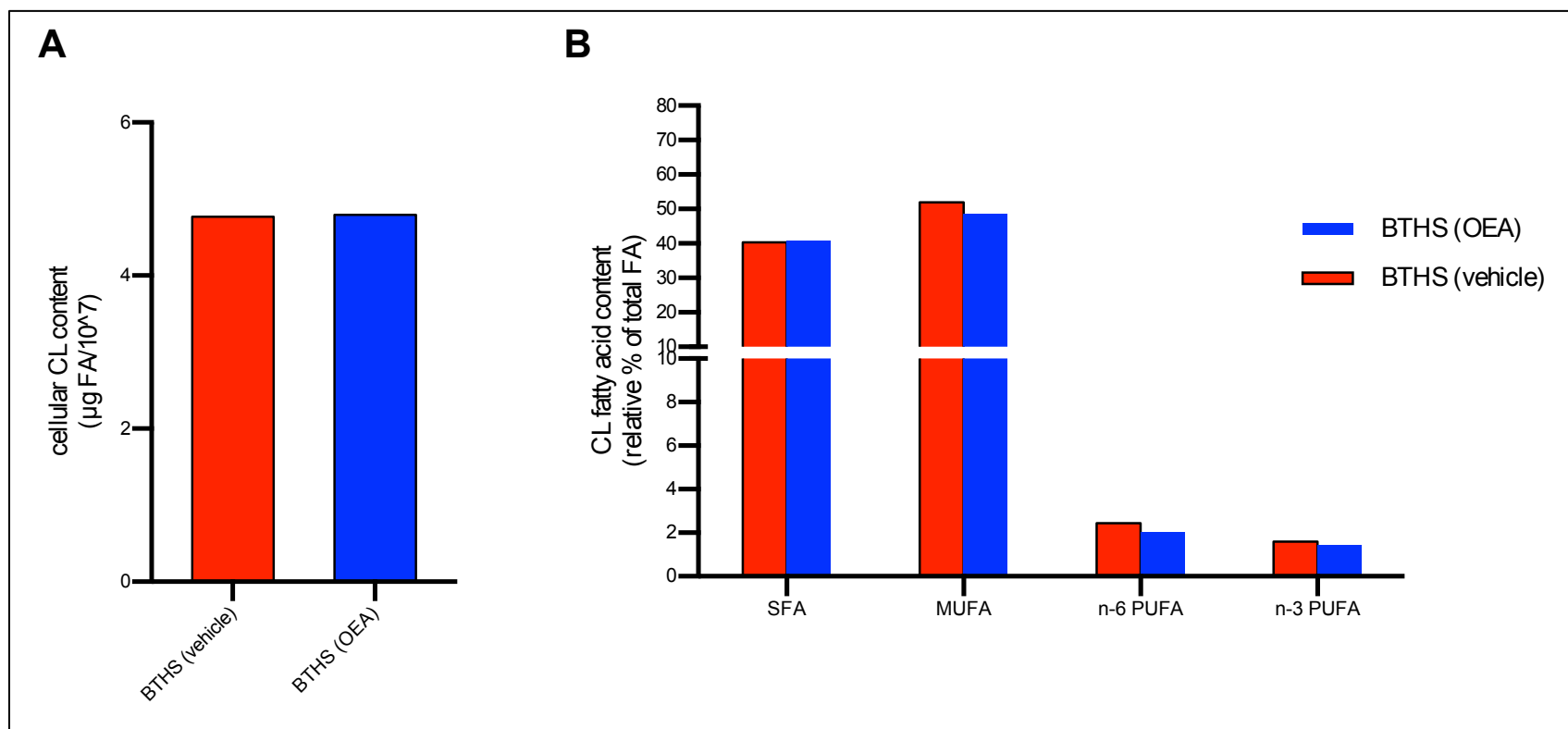


Appendix figure 2: Technical replicates of the growth data of each individual BTBS and healthy lymphoblast donors, treated with LEA or vehicle.

(A-C) represents technical reps of GM22192 (BTBS) & AG15022 (healthy), (D-E) represents technical reps of GM22194 (BTBS) & AG14947 (healthy), (F-G) represents a single technical rep of GM22193 (BTBS) & AG14731 (healthy), and GM22150 (BTBS) & AG14948 (healthy).

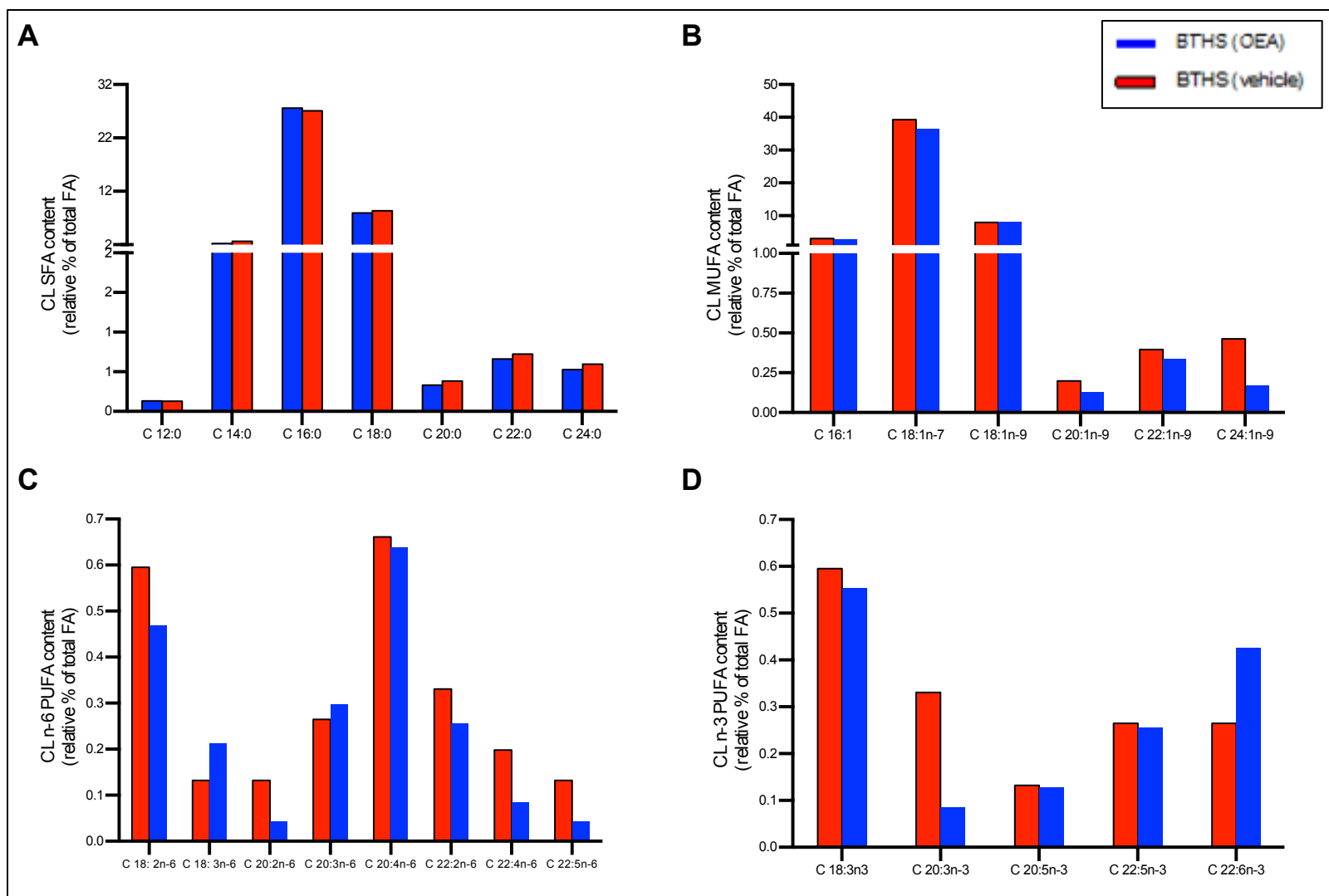
Appendix Table 1: Absolute mass of individual fatty acyl species within the CL of GM22163 (BTHS) and AG14750 (healthy) in micrograms per 10 million cells ($\mu/10^7$ cells).

<i>Fatty Acid</i>	<i>Healthy (vehicle)</i>	<i>Healthy (OEA)</i>	<i>Barth (vehicle)</i>	<i>Barth (OEA)</i>
<i>C 12:0</i>	0.002	0.002	0.003	0.003
<i>C 14:0</i>	0.105	0.097	0.077	0.065
<i>C 16:0</i>	0.725	0.693	1.275	1.133
<i>C 18:0</i>	0.222	0.236	0.369	0.318
<i>C 20:0</i>	0.015	0.011	0.009	0.014
<i>C 22:0</i>	0.010	0.009	0.015	0.014
<i>C 24:0</i>	0.015	0.011	0.018	0.017
<i>SFA total</i>	1.109	1.071	1.790	1.581
<i>C 16:1</i>	0.887	0.938	0.089	0.082
<i>C 18:1n-7</i>	1.311	1.379	1.406	1.271
<i>C 18:1n-9</i>	0.723	0.841	0.256	0.251
<i>C 20:1n-9</i>	0.007	0.004	0.009	0.011
<i>C 22:1n-9</i>	0.015	0.011	0.006	0.014
<i>C 24:1n-9</i>	0.017	0.007	0.015	0.011
<i>MUFA total</i>	2.970	3.190	1.788	1.648
<i>C 18:2n-6</i>	0.256	0.263	0.015	0.014
<i>C 18:3n-6</i>	0.007	0.002	0.009	0.006
<i>C 20:2n-6</i>	0.005	0.002	0.012	0.006
<i>C 20:3n-6</i>	0.081	0.088	0.006	0.008
<i>C 20:4n-6</i>	0.029	0.029	0.033	0.034
<i>C 22:2n-6</i>	0.010	0.013	0.012	0.020
<i>C 22:4n-6</i>	0.015	0.004	0.006	0.008
<i>C 22:5n-6</i>	0.012	0.007	0.015	0.008
<i>N-6 PUFA total</i>	0.415	0.409	0.107	0.104
<i>C 18:3n-3</i>	0.020	0.022	0.027	0.028
<i>C 20:3n-3</i>	0.007	0.004	0.006	0.006
<i>C 20:5n-3</i>	0.010	0.004	0.012	0.006
<i>C 22:5n-3</i>	0.010	0.013	0.015	0.017
<i>C 22:6n-3</i>	0.010	0.011	0.018	0.017
<i>N-3 PUFA total</i>	0.056	0.056	0.077	0.073



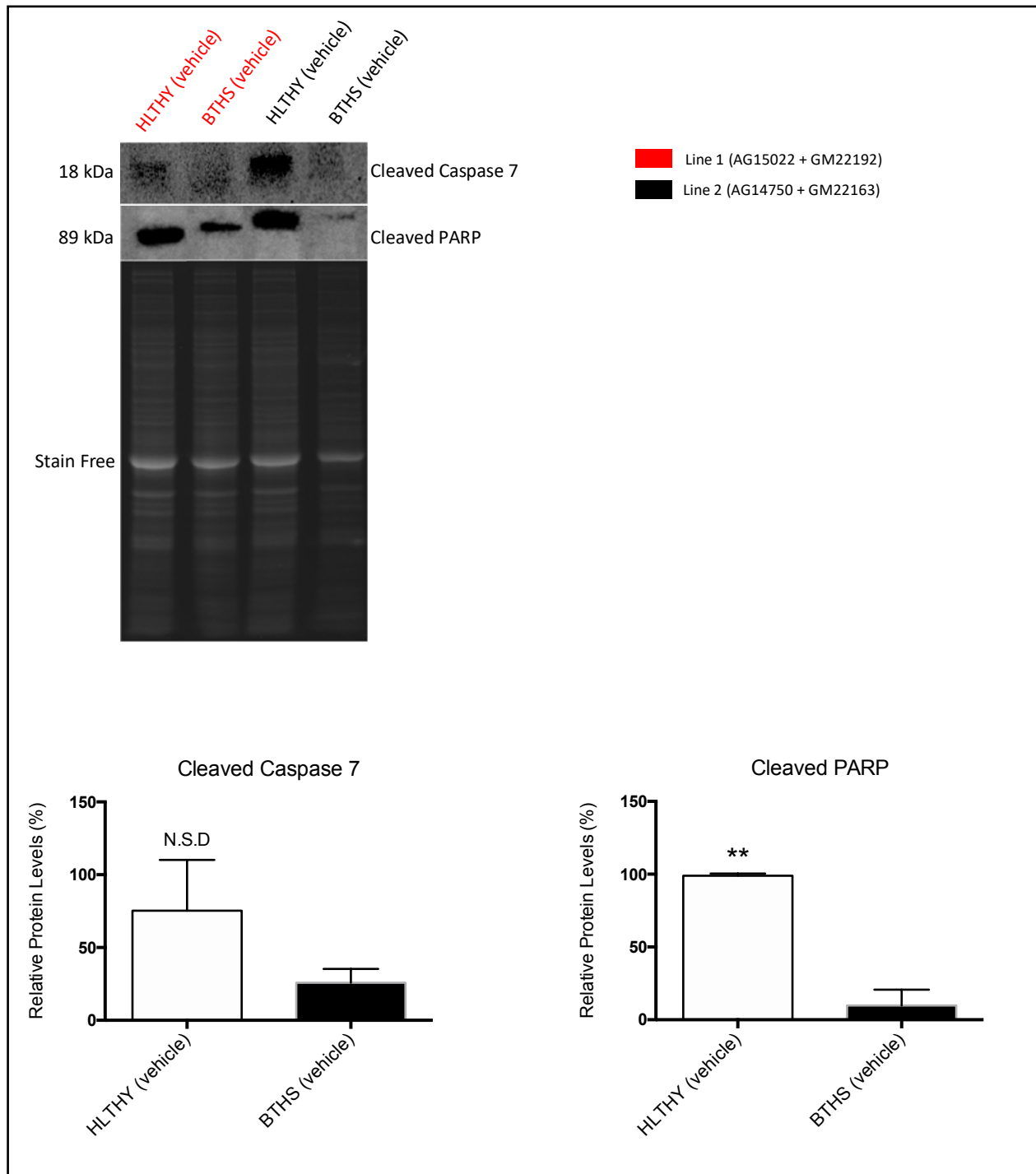
Appendix figure 3: Preliminary cardiolipin analysis of a single BTHS lymphoblasts cell line (GM22192), treated with OEA or vehicle.

(A). Endogenous CL content of lymphoblast derived from BTHS treated with vehicle or OEA for 96 hours. (B) Relative % of major fatty acid classes (i.e. SFA, MUFA, PUFA) within CL from BTHS lymphoblast treated with either OEA or vehicle.



Appendix figure 4: Fatty acyl profile of CL isolated from a single BTHS lymphoblast line (GM22192) treated with or without OEA.

Relative proportions of individual fatty acyl species within CL from cultured BTH lymphoblasts treated with vehicle or OEA for 96 hours. (A) SFA species, (B) MUFA species, (C) n-6 PUFA species, (D) n-3 PUFA species.



Appendix figure 5: Relatively lower protein levels of cleaved caspase 7 and cleaved PARP in BTHS lymphoblasts compared to healthy controls. N=2, data are represented as relative percentage \pm S.E.M